IMPACT OF ACUTE ETHANOL INJECTIONS ON MEDIAL PREFRONTAL CORTEX NEURAL ACTIVITY

by

Mitchell D. Morningstar

A Thesis

Submitted to the Faculty of Purdue University

In Partial Fulfillment of the Requirements for the degree of

Master of Science

Department of Psychology at IUPUI

Indianapolis, Indiana

December 2019

THE PURDUE UNIVERSITY GRADUATE SCHOOL
STATEMENT OF COMMITTEE APPROVAL

Dr. Christopher Lapish, Chair

Department of Psychology

Dr. David Linsenbardt

Department of Psychology

Dr. Charles Goodlett

Department of Psychology

Approved by:

Dr. Cristine Czachowski

TABLE OF CONTENTS

LIST OF TABLES

LIST OF FIGURES

ABSTRACT

The medial prefrontal cortex (mPFC) is a cortical brain region involved in the evaluation and selection of motivationally relevant outcomes. mPFC-mediated cognitive functions are impaired following acute alcohol exposure. In rodent models, ethanol (EtOH) doses as low as 0.75 g/kg yield deficits in cognitive functions. These deficits following acute EtOH are thought to be mediated, at least in part, by decreases in mPFC firing rates. However, these data have been generated exclusively in anesthetized rodents. To eliminate the potentially confounding role of anesthesia on EtOH modulated mPFC activity, the present study investigated the effects of acute EtOH injections on mPFC neural activity in awake-behaving rodents. We utilized three groups: the first group received 2 saline injections during the recording. The second group received a saline injection followed 30 minutes later by a 1.0 g/kg EtOH injection. The last group received a saline injection followed 30 minutes later by a 2.0 g/kg EtOH injection. One week following the awake-behaving recording, an anesthetized recording was performed using one dose of saline followed 30 minutes later by one dose of 1.0 g/kg EtOH in order to replicate previous studies. Firing rates were normalized to a baseline period that occurred 5 minutes prior to each injection. A 5-minute time period 30 minutes following the injection was used to compare across groups. There were no significant differences across the awake-behaving saline-saline group, indicating no major effect on mPFC neural activity as a result of repeated injections. There was a significant main effect across treatment & behavioral groups in the saline-EtOH 1.0 g/kg group with reductions in the EtOH & Sleep condition. In the saline-EtOH 2.0 g/kg, mPFC neural activity was only reduced in lowered states of vigilance. This suggests that EtOH only causes gross changes on neural activity when the animal is not active and behaving. Ultimately this means that EtOH's impact on decision making is not due to gross changes in mPFC neural activity and future work should investigate its mechanism.

INTRODUCTION

mPFC structure and function

The medial prefrontal cortex (mPFC) is a cortical brain region involved in the evaluation and selection of motivationally relevant outcomes. The mPFC functions as an action-outcome evaluator and predictor (Alexander, 2011); it integrates inputs from subcortical, neuromodulatory, and sensory regions (Euston, 2012), and then evaluates them in the context of memories (Tamura, 2017). Functionally, this allows for top-down control over behavior that is necessary for optimal decision making. This makes the mPFC important in a wide range of diverse behaviors including, but not limited to, social cognition (Franzen & Myers, 1973), processing and understanding pain (Jahn, 2016), cognitive and inhibitory control (van Gaal, 2008), memory consolidation (Tang, 2017; Rothschild, 2017), regulating fear learning (Gentry, 2018), and reward seeking (Gutman, 2017). It accomplishes these disparate tasks through precise control of neural ensembles (Onos, 2016; Moorman 2015) and can flexibly and adaptively switch between these ensembles to exert top-down control over decision making (Malagon-Vina, 2018). Given the important and ubiquitous nature of the mPFC in behavioral selection, tight regulation of activity in mPFC is necessary for executive cognitive function.

Structurally the mPFC is made up of three anatomically distinct subregions: the anterior cingulate (Cg1), prelimbic (PL), and infralimbic (IL) (van Eden, 1985). These subregions then exhibit functional differences along the dorsal-ventral axis. Cg1 and dorsal portions of the PL make up the dorsal mPFC while ventral portions of the PL and IL make up the ventral mPFC (Berendse, 1993). The dorsal mPFC is broadly responsible for the integration of present and past information as well as affective states while the ventral mPFC is associated with integration of visceromotor responses (Vertes 2004). Projections from the PL are found in a diverse range of brain regions such as the insular cortex, claustrum, nucleus accumbens, olfactory tubercle, thalamus, and dorsal/median raphe nuclei. While there is some minor overlap between projections of the PL and IL, the IL mainly projects to various subregions in the basal forebrain, amygdala, hypothalamus, and brainstem (Vertes 2004). Functionally the PL is thought to be involved in goal-seeking behaviors while the IL is thought to be involved in habitual responding. (Killcross, 2003; Vidal-Gonzalez, 2006). Additionally, it has been hypothesized that the PL

facilitates acquisition of a fear response while the IL facilitates inhibition of the fear response during extinction (Morgan 1995). This led to the hypothesis that the PL leads to the execution of a behavior while the IL leads to inhibition. This was then extrapolated to drug-seeking versus drug-extinction (Moorman and Aston-Jones, 2015). However, more recent findings have suggested that the functional delineation between the two subregions is more complex and both the PL and IL encode context specific information regarding stop/go signals in the presence of a natural reinforcer (Moorman, 2015; Riaz, 2019). Collectively, this suggests that while there are appreciable functional differences based on each subregion's projections (Vertes, 2004) and physiology (Gretenkord, 2017), both subregions are necessary for the execution of complex behaviors. Specific to the present study, the dorsal mPFC (comprising the dorsal portions of the PL as well as Cg1) is well studied in EtOH research and was chosen for its role in alcohol seeking behaviors (Linsenbardt, 2015; Linsenbardt, 2019; Khoo, 2019) as well as to compare our data with previous studies on *in vivo* mPFC activity in response to EtOH (Tu, 2007). The present study defines the dorsal mPFC as containing the dorsal PL and all of Cg1.

The mPFC also exhibits differences between layer 2/3 and layer 5 neurons. For example, chronic intermittent EtOH exposure (CIE) alters dendrite morphology in layer 2/3 of the PL subregion but not the IL subregion. Consistent with this observation, layer 2/3 PL neurons also exhibit enhanced glutamatergic transmission, and this was correlated with enhanced performance in the Barnes Maze indicating greater spatial learning and memory (Varodayan, 2017). mPFC's layer 2/3 and 5 neurons also exhibit differences in their biophysical properties. Layer 5 neurons are more excitable than layer 2/3 neurons while layer 2/3 neurons in the IL are more excitable than their counterparts in the PL (Song, 2017). Calcium electrogenesis, a potential mechanism of coincidence detection in neural firing relevant for Hebbian learning, has also been found to occur differentially in layer 2/3 versus 5 neurons with a higher proportion of layer 5 neurons exhibiting calcium electrogenesis (Zimbo, 2013). The general model of layer specific activity in the mPFC is thought to go as such: layer 2/3 neurons control the gain of an input (Quiquempoix, 2018) and contextualize and integrate it with information about the present state of the organism. Layer 5 neurons then send out the sum of the integrated information to downstream targets (Petersen, 2013; Crochet, 2009). Differences in morphological and biophysical properties of neurons in each layer allow for these specializations (van Aerde, 2013) and cannot be discounted when interpreting cortical results.

Functionally, layer 2/3 pyramidal neurons are involved in corticocortical (Quiquempoix, 2018) loops while layer 5 pyramidal neurons are involved in corticothalamic and corticostriatal loops (Crochet, 2009) depending on pyramidal cell type. Nakayama (2018) recently investigated the functional differences of these pathways using an optogenetic model that specifically targeted either corticocortical loops, corticothalamic loops, or corticostriatal loops. Additionally, they non-specifically inhibited the mPFC by stimulating local interneurons. In a probabilistic discounting task, they found that corticothalamic and corticostriatal loops are recruited in situations requiring cognitive flexibility while corticocortical loops had no effect on their task. Non-specific mPFC inactivation via interneuron stimulation resulted in increases of impulsivity and compulsivity reflected in premature responses and choice bias. These results suggest that mPFC circuits are differentiallyy recruited for aspects of tasks requiring cognitive flexibility and executive function.

Impairments in cognitive function and control are found after lesions of the mPFC and lead to behavioral inflexibility and sub-optimal decision making in paradigms such as the Iowa Gambling Task. Patients with mPFC damage were unable to accurately estimate the probability of reward in a series of decks of cards, whereas healthy patients or patients with damage in other brain areas were able to accurately learn what the task's contingencies were and reliably choose the most advantageous strategies (Bechara et al., 1994). In addition to mPFC's importance in decision making, mPFC lesions in rhesus monkeys led to declines in social behavior and ultimately ostracism from their social groups resulting in isolation and death (Franzen and Myers, 1973). Last, patients with mPFC damage experienced dulled emotional responses to images of threatening or disturbing stimuli (Damasio, 1994). Without the executive, top-down control of the mPFC, higher-level organisms are unable to make optimal decisions, properly valuate emotional stimuli in their environment, and maintain acceptable social norms.

Understanding how and if the rodent and primate mPFC are homologous is an intensely debated subject. The primate dorsolateral prefrontal cortex (dlPFC) is observed to be the nexus of many high-level executive functions (Preuss, 1995). The primate dlPFC has four important, broad categories that aid cognitive control. Selective attention, working and short-term memory, updating information, and shifting attention (Brown, 2002). The rodent mPFC is functionally able to carry out these four categories despite anatomical incongruence with primate dlPFC

(Preuss, 1995). Anatomically and evolutionarily, the rodent mPFC is most congruent with a separate area of the primate PFC: the agranular anterior cingulate cortex (ACC) (Laubach, 2018). Ultimately the rodent mPFC is functionally homologous to the primate dlPFC while being anatomically homologous to the primate ACC. This suggests that rodent mPFC can carry out computations that are functionally relevant to primate dlPFC despite lacking a granular mPFC, and this ultimately leads to the instantiation of behaviors related to the four broad categories of cognitive control described above.

Effects of EtOH on mPFC Mediated Behaviors

mPFC maladaptation also occurs following chronic alcohol use in both rodent (Trantham-Davidson, 2014) and human populations (Seo et al., 2013). These neuroadaptations can be functionally similar to what is observed following mPFC damage. Alcohol related dysregulation of the mPFC contributes to a decline in cognitive control, resulting in elevated saliency of alcohol related cues (Bechara, 2005), impairment in delayed discounting, a blunted response to rewards (Forbes, 2014), and heightened emotional impulsivity (Cyders 2014). This mixture of effects makes it particularly difficult for patients with alcohol use disorder (AUD) to overcome the urge to drink (Bechara, 2005). Utilizing functional magnetic resonance imaging (fMRI), it has been shown that this decline in cognitive control is correlated with an elevation of mPFC neural activity during resting state scans. Importantly, this elevation of mPFC activity is predictive of relapse (Seo et al., 2013). This heavily implicates mPFC hyperactivity in having a crucial and active role in the EtOH mediated effects on cognition.

In agreement with the effects of chronic alcohol use, acute EtOH exposure also produces deficits in cognition, particularly in spatial memory tasks, at doses as low as 0.75 g/kg (Givens, 1995; Ketchum, 2016; Chin, 2011). These acute cognitive effects are prominently seen in the Morris Water Maze (Matthews 2000), radial arm maze, and contextual conditioned fear responses (Kutlu, 2016). One possible mechanism responsible for the decline in spatial memory is a deficit of hippocampal place cell specificity. Place cells that are normally active only in specific zones of a radial arm maze become non-specifically active throughout several compartments of the maze (Matthews 2002).

One additional behavior reliably affected by acute EtOH is the expression of contextually conditioned fear responses. Contextually conditioned fear responses can be broken down into trace and delay conditions. Trace conditions are both amygdala and hippocampal dependent while delay conditions are mostly only amygdala dependent. EtOH has differential effects on these two experimental regiments (Van Skike et al, 2019). Trace conditioning is impaired following EtOH pretreatment during training, while delay conditioning is mostly unaffected. This suggests that EtOH is disrupting learning in the trace conditioning experiments (Hunt et. al., 2009). However, experimental conditions may greatly impact the results. For example, Gulick (2008) found deficits in both contextual and cued responses following pre-training EtOH in a delayed conditioning model. This suggests that specific experimental parameters may be a critical component of whether acute EtOH has an impact on behavior.

Rodent models of delayed discounting may also be impaired by EtOH, resulting in a decreased desire to wait for a delayed but larger reward (Wit, 2009). However, the effects of EtOH on delayed discounting in rodent models appears to be dose, strain, and contingency dependent and does not always reliably produce deficits (Wilhelm 2012). An additional area of exploration within the acute EtOH field is the novel object recognition task. An animal is placed within an arena and allowed to explore two novel objects. The animal and one of the objects are then removed at the conclusion of the initial exploration phase. A new, novel object replaces one of the old familiarized objects and the animal is returned to the arena after a specified time period. Evidence of novel object recognition comes via greater time spent exploring the new, novel object versus the old, familiarized object. Studies have indicated that the mPFC is activated during this task (Tanimizu, 2018) and that dopamine D1 receptors within the PL subregion have an important role in the encoding and retrieval of object memory (Pezze, 2014). Acute EtOH has been shown to reliably decrease object exploration subsequently leading to deficits in the novel object recognition task (Ryabinin, 2002) and the impairments caused by acute EtOH can then be rescued using an mGlu5 receptor positive allosteric modulator (Marszalek-Grabska, 2018).

The inconsistencies described above suggest that behavioral models of the effects of acute EtOH on cognition in rodents are difficult to design and implement, however, an overall picture emerges. Learning is task dependently impaired with EtOH pre-treatment and is most apparent in spatial memory tasks and trace conditioned fear responses. While the mPFC is

involved in many of these tasks, the role of the mPFC was not explicitly tested in all of them. Given the mixed results seen in these tasks, refined behavioral models must be developed for evaluating acute EtOH's effects on mPFC specific processes.

Although results from rodent models of EtOH's effects on cognitive processes have been mixed, human models are clearer. Moderate EtOH doses in humans have been shown to lead to deficits in the Stroop task (Marinkovic, 2012) and working memory tasks (Gundersen, 2008) that are moderated by mPFC activity. Weissenborn (2002) showed both a decrease in working memory as well as an increase in impulsivity following orally consumed EtOH. Participants in the alcohol condition (0.8 g/kg) took more moves to reach criterion and made choices faster, resulting in a greater number of errors. Working memory is specifically altered via decreasing the efficacy of mnemonic strategies and executive processes without altering overall working memory capacity (Saults, 2007). While the overall working memory capacity may not be altered, in individuals with a lower baseline working memory capacity, EtOH reduces working memory's ability to inhibit responses. Again, this leads to greater impulsivity (Finn, 1999). EtOH has a clear role in reducing human use of working memory and increasing impulsivity. However, it is difficult to assess acute EtOH activity in humans due to differences in alcohol history. Impairments in cognitive function following acute EtOH exposure are alcohol history dependent due to prior alcohol history producing tolerance (Boulouard, 2002; Wright, 2013). Discovering the neural circuits most disrupted by acute EtOH will be critical in understanding how chronic EtOH alters them in AUD.

Spike-trains

In the present work, we analyzed and found instances of action potentials in our extracellular signal and preserved the time-points in which they occurred. These timepoints are known as the spike-train for a given neuron. Spike-train analysis has led to many novel findings in neuroscience ranging from visual receptive fields, where a visual neuron's activity is dependent on a specific line orientation, (Hubel and Wiesel, 1959) to predictive encoding of a reward, where dopaminergic neurons increase their firing rates prior to the delivery of a learned reward (Schultz, 1998). Beyond reward-prediction and receptive fields, neurons are also capable of transmitting information about specific features of the environment such as faces, objects, and

landmarks; for example, a single neuron may exhibit an increased firing frequency when presented different photographs of Jennifer Aniston's face (Quiroga, 2005). These studies have provided evidence that spike-trains are encoding information about external stimuli ranging from general stimuli such as line orientations to more specific stimuli such as faces and places. Additionally, these studies have historically provided evidence for representational theories of neural function where a specific bit of information is maintained using specific subsets of neurons (Simon and Newell, 1970). While the field is moving towards population level representations found using dimensionality reduction techniques (Saxena, 2019; Kalaska, 2019), the same basic tenants apply: information is encoded in the frequency and firing modality of neurons, which then makes spike-trains the basic unit of that information encoding.

Spike-train analyses have been critical in our understanding of reward pathways and how they go awry in addiction to drugs of abuse. For example, electrophysiological evidence has pointed to differential functions in the NAc core and shell (Wood, 2011), and has also shown that prolonged periods of cocaine use can blunt striatal activity necessary for associative learning tasks (Saddoris, 2014). Additionally, electrophysiological studies have shown that the subthalamic nucleus (STN) is a critical encoder of positive and negative valences in the striatum and exhibits prediction-error signals similar to other striatal areas (Breysse, 2015). These analyses have allowed us to test the function of various brain regions and how that function is altered following development of psychological disorders. Specific to AUD, selectively bred alcohol-preferring P-rats have been shown to have an enhanced response in mPFC neural activity while drinking compared to their progenitor Wistar controls (Linsenbardt, 2015). Additionally, while the overall response is enhanced, the neural correlate of drinking intent is blunted (Linsendbardt, 2019). Overall, investigating the neural correlates of decision making via spike-train analyses is a critical first step in understanding how decision making goes awry (or away) in progressive biopsychological pathologies such as AUD and addiction.

Acute Electrophysiological Effects of Ethanol on mPFC

It has been hypothesized that a reduction in mPFC firing rates is responsible for the cognitive declines observed following acute EtOH. Tu et. al. (2007) showed a dose-dependent decrease in spontaneous firing rates of the mPFC following acute EtOH exposure in both

anaesthetized *in vivo* recordings as well as in *in vitro* slice preparation. Importantly, the decreases in persistent activity found in anesthetized animals and slice-preparation were within the context of cortical up-states and down-states induced via urethane anesthesia. While an animal is under urethane anesthesia, neural firing almost exclusively takes place during depolarized cortical up-states while cortical down-states are hyperpolarized periods of time in which no activity occurs. This means that the duration and frequency in which up-states occurred was depressed by EtOH which resulted in a net total decrease in spontaneous firing rates. These alterations in up-states were dependent on EtOH dosage and contributed to the net decrease in firing rates observed in Tu et. al. (2007). However, cortical up-states and down-states are only found naturally during deep sleep (Sanchez-Vives, 2010) and are otherwise induced and modulated by the dosage of certain anesthetic agents (Dao Duc, 2015). For example, a deeper level of urethane anesthesia will produce similar decreases in up-state frequency and duration as EtOH (Dao Duc, 2015). Therefore, it is possible that the effects observed were only EtOH mediated modulations of urethane anesthesia and not purely an effect of EtOH.

Previous research has directly compared the effect of anesthetic choice (halothane, chloral hydrate, local anesthesia, and urethane) on alcohol's actions in the cerebellum. When urethane anesthesia was used, a sharp decrease in cerebellar spontaneous neural activity was seen after EtOH exposure. However, for all other anesthetics tested, EtOH excited neural activity in the cerebellum (Siggins et. al., 1987). While urethane exerts influence over many ligand-gated ion channels, it has no specific affinity towards either inhibition of excitatory ion channels such as NMDA or potentiation of inhibitory ion channels such as GABA. This contrasts to other widely used anesthetic agents that have higher affinities for one system over the other. Hara and Harris (2002) noted this and concluded in their study that the anesthetic most similar to urethane is EtOH given that it acts to both inhibit NMDA channels and facilitate GABAergic transmission. Ultimately it is difficult to conclude that EtOH induced decreases in firing rates are responsible for deficits in decision making. This is due to the potential of urethane and EtOH to have synergistic effects. Additionally, most effects have been found in the context of a cortical state that is only naturally found in sleep (Whitten, 2009). While urethane is an overall useful anesthetic agent, it may have extra confounds while studying EtOH given their pharmacological similarities.

Beyond anesthetized preparations, slice preparations have been widely used to measure acute EtOH's effects on mPFC spontaneous or evoked activity. Crucially, *in vitro* slice preparations of mPFC cells exhibit similar up-down states as *in vivo* anesthetized preparations (Tu et. al. 2007). EtOH has been found to decrease up-state amplitude, duration, and spiking frequency in a dose dependent manner (Tu, et. al. 2007). Furthermore, the alterations in up-state behavior were found to be NMDA receptor dependent (Weitlauf, 2008). Subsequent investigation into fast-spiking interneurons found that NMDA blockade was not sufficient to affect fast-spiking interneurons. Despite this, EtOH was able to inhibit both fast-spiking interneurons and pyramidal neurons suggesting that up-states are a product of network-level connections that are robustly affected when EtOH enters the system (Woodward, 2009). Follow up experiments using calcium imaging suggest that EtOH alters up-states on a network level, and this inhibition is chiefly the product of NMDA receptor antagonism induced via EtOH (Woodward, 2012). In contrast, $GABA_A$ and AMPA receptors (receptors that are equally important for up-state dynamics) were not affected by the concentrations of EtOH used in the previously mentioned studies (Weitlauf, 2008). This again suggests that the NMDA receptor is the primary target of EtOH's actions in mPFC slice preparations. Slice preparations have yielded an impressive knowledge as to how EtOH is altering the dynamics of up-states. However, it is unclear how the altered neural dynamics of up-states can reliably be translated to how EtOH impacts the neural dynamics of awake-behaving states necessary for cognition.

Given these confounds, it is crucial for additional electrophysiological studies of EtOH's actions on the mPFC to be conducted in awake and behaving animals. Linsenbardt (2015) investigated mPFC activity in alcohol-preferring "P" versus Wistar rats in a Pavlovian alcohol consumption task and found no correlation between alcohol intake and firing rates in the mPFC. Importantly, these animals were awake-behaving and voluntarily consuming alcohol to the point of intoxication. It is also important to mention that these animals received multiple doses of alcohol over the course of a few days which may have resulted in short term neuroadaptations in firing rates. Despite this, it is evident that under these conditions, EtOH is not acting on the mPFC in a manner consistent with how it acts under urethane anesthesia.

Electrochemical and microdialysis approaches also suggest that EtOH in awake-behaving animals may have drastically different effects as compared to those in anesthetized animals. For

example, no decreases in mPFC glutamate have been found in EtOH naïve, mature, and freely moving animals receiving an acute injection of alcohol (Selim 1996; Mishra 2015). This complicates the findings of previous literature that suggests EtOH disrupts glutamate receptor function *in vitro* (Lovinger, 1990). It also complicates suggestions that NMDA receptor antagonism is critical for dose dependent decreases of spontaneous activity during *in vivo* anaesthetized animal recordings or *in vitro* slice preparations (Weitlauf, 2008). It is thus apparent that at both levels of neurotransmission and electrophysiology, EtOH has a different effect on the mPFC in awake-behaving animals compared to anaesthetized animals and slice preparations.

Specific Hypotheses

The present study aims to contrast the effects of EtOH on the mPFC in awake-behaving animals with its effects in anesthetized animals. This study is an important first step in identifying potential mechanisms underlying acute deficits on cognition following EtOH exposure as well as how these acute deficits progress into long-lasting changes in AUD. It is hypothesized that EtOH at 1 g/kg will preserve spontaneous firing rates in the awake-behaving condition while decreasing spontaneous firing rates in the anesthetized condition. EtOH at a higher dose such as 2 g/kg will produce decreases in spontaneous firing rates in the awake-behaving condition but not at the same magnitude as what is seen anesthetized experiments.

METHODS

Animals

A total of 76 adult, male outbred Wistar rats (Harlan – IN) with weights ranging from 300-450g and ages ranging from 2-4 months were used throughout this experiment. 28 animals were utilized to measure the impact of acute EtOH injections on mPFC neural activity while the remaining 48 animals were utilized to characterize alcohol metabolism. Animals excluded from the study for any reason are described in **Figure 1**. All animals were initially single housed in opaque, plastic cages with pine bedding. Animals who underwent surgical operations were moved to translucent, standard plexiglass cages with "Yesterday's News" bedding. Animals were kept on a reverse light cycle such that all testing occurred during their dark phase. All experiments were approved by Indiana University-Purdue University Indianapolis' (IUPUI) Institutional Animal Care and Use Committee (IACUC).

Apparatus

An opaque open field (40.64 cm x 40.64 cm x 38.1 cm) was used for all recordings. A Doric Commutator (Doric Lenses – Canada) was placed above the open field in order to allow the rat to explore and move freely. An OpenEphys (OpenEphys – MA) acquisition system was used to collect all electrophysiological data. AnyMaze (ANY-maze Behavioral tracking software – UK) was used to collect all behavioral and locomotor data.

Surgical Procedures

Animals were first anesthetized under isoflurane (2.5% at 4 L/h for induction, 2% at 1.0 L/h for maintenance). Fur was removed from the skull using a set of Oster clippers. Following this, animals were placed in the stereotaxic equipment and checked for spinal reflexes. After loss of spinal reflexes, the area of incision was sanitized using a 70% ethyl alcohol solution and iodine. Following sanitation of the incision area, the local anesthetic Marcaine was applied (5 mg/kg, s.c.). Artificial tear ointment was placed on the animals' eyes. A circular incision was made in order to expose the skull. Extra connective tissue was removed if necessary, the skull was cleaned, and bregma-lambda coordinates were found. mPFC coordinates were then found

(AP: 2.8, ML: 0.3, DV: 3.0 from brain) and marked using a sanitized graphite pencil. 7 holes were drilled for either ground screws (2) or anchoring screws (5). Stainless steel screws were placed in these respective holes prior to beginning probe implantation. A rectangular craniotomy was performed around the coordinates of the mPFC that measured no more than 4 mm in length and 2 mm in width. Following the craniotomy, the dura was removed, and the insertion site was cleared of any blood or bone fragments using a sterile saline preparation. Excess saline was removed, and an artificial dura silicon polymer solution was applied to the craniotomy site (Cambridge Neurotech – Cambridge England). The probe was then placed on the stereotax and lowered until it reached brain tissue. The center of the probe was placed at the mPFC coordinates and then slowly lowered to the target. At the conclusion of the probe's descent, dental cement was first applied to the area surrounding the probe insertion. Once hardened, ground wires were soldered to the electronic interface board (EIB) of the probe. After completion of the ground wire soldering, the probe and any exposed skull was encased in dental cement. The analgesic ketoprofen (5 mg/kg, s.c.) and the antibiotic cefazolin (30 mg/kg, s.c.) were given while the dental cement dried. Isoflurane was then cut, and the animal was given pure oxygen for 5 minutes while recovering from the anesthetic. At the conclusion of these 5 minutes, the animal was placed in a heated recovery cage until recovery of its righting reflex. Following recovery of the righting reflex, the animal was placed inside a transparent plexiglass cage with an inverted lid, "Yesterday's News" bedding, and wet breeders chow. The animal was returned to the colony room and monitored for 7 days post-surgery.

Electrophysiological Equipment

Custom built 32 channel microwire arrays (MWA) were constructed using 23 μm diameter tungsten wires, an in-house fabricated electronic interface board (EIB), and an in-house fabricated wire array made of 100 μm diameter silicon tubing. A male Omnetics (Omnetics – MN) connector was soldered to a manufactured copper circuit board (PCB) in order to create our EIBs. The wire array was fabricated by epoxying together 2 rows of 16 silicon (100 μm diameter) tubes to create a 16x2 array to house all 32 wires. On experimental days, surgically implanted probes were connected to an Intan Omnetics headstage (Intan – CA) in order to amplify the analog signal and convert it to a digital signal compatible with OpenEphys. The converted signal traveled through a chain of Intan SPI cables until reaching the OpenEphys

acquisition box. Data was streamed from the OpenEphys acquisition box to a compatible desktop computer via a USB 2.0 connection and sampled at 30 kHz. The raw signal output of the extracellular recordings was saved onto this desktop computer, backed up to both an external hard drive and Box. Locomotor data was concurrently collected using OpenEphys via an analog-to-digital port (ADC). Analog locomotor data was output via AnyMaze software and AnyMaze's AMi-2 analogue interface, input to OpenEphy's ADC port, and sampled at 30 kHz in OpenEphys.

Blood Ethanol Concentration Curve

A blood ethanol concentration (BEC) curve was generated using a cohort of 48 adult, male Wistars in both awake-behaving and anesthetized conditions. In the anesthetized condition, animals were first anesthetized using 1.5 g/kg of urethane. Animals were weighed and then given either a dose of 1.0 g/kg EtOH or 2.0 g/kg EtOH. A small incision was made at the tip of the animal's tail and 50 µL of blood was sampled at 5, 15, 30, 60, and 90 minutes post-EtOH injection. Blood samples were chilled and spun at 15,000 RPM for 5 minutes to separate red blood cells from plasma. Plasma was collected and frozen at -20C until analyzed using an Analox machine and Analox alcohol reagent kit (Analox Instruments Ltd. – UK).

Upon acquisition of BEC values, data was imported and analyzed in MATLAB. A custom function was fit to the data using MATLAB's non-linear regression function fitnlm. This allowed us to reliably estimate BEC values for each EtOH dose throughout the entire time course of the electrophysiology recording. This informed recording length and data analysis.

Awake Behaving Recordings

Three separate surgery cohorts were tested (see **Figure 1** or **Table 2**). Test days occurred at least 1 week following each animal's surgery date. All testing was conducted under red light in order to not disrupt the animal's light cycle. At the beginning of each test, the animal was weighed and doses for either saline, 1.0 g/kg EtOH, or 2.0 g/kg EtOH were calculated. The animal was then connected to the electrophysiological acquisition system and allowed to habituate to the open field container and headstage for a period of 15 minutes. Following the 15-minute period, the animal was returned to its home cage and acclimated to the testing room for 4

hours. After 4 hours, animals were reconnected to the acquisition system and placed inside of the open field. Data acquisition began once the animal was seen to have a stable connection free from any major electrical artifacts. A baseline recording period of at least 10 minutes was acquired. Following the baseline recording period, the animal received its first injection. For Groups 1 and 2, the saline injection was volume matched to a 1.0 g/kg dose of EtOH. For Group 3 the saline injection was volume matched to a 2.0 g/kg dose of EtOH. A period of 30 minutes followed this first injection and the animal was then given a second injection. For Group 1, the second injection was additional saline. For Group 2 the second injection was 1.0 g/kg of EtOH. For Group 3, the second injection was 2.0 g/kg of EtOH. Following the second injection, the recording continued for 2 hours. On average this resulted in a recording that lasted 166 minutes in total from baseline to the end. At the end of the recording, a small incision was made at the tip of the tail and 100 μL of blood was drawn from animals who received EtOH. This blood was subsequently handled as described in the previous section.

Anesthetized Recordings

Anesthetized recordings took place at least 1 week after the awake-behaving recordings described above. Animals were weighed and doses for urethane (1.5 g/kg), saline, and EtOH (1.0 g/kg) were calculated. Animals were then anesthetized and connected to the acquisition system. After cessation of spinal reflexes, the recording period began. A baseline period of at least 10 minutes was collected prior to any experimental manipulations. Following the baseline period, a saline injection volume matched to 1.0 g/kg of EtOH was given and a period of 30 minutes post-saline was recorded. Following this 30-minute period, an EtOH dose of 1.0 g/kg was given to all animals. A recording period of at least 2 hours followed this EtOH injection. Tail bloods were taken at the conclusion of the recording period in order to assess BEC.

Histology

Following the anesthetized recording, a 10 mA current was applied to each connector on the EIB in order to create a lesion at the tips of the MWA for histological verification. After lesioning, animals were once again checked for spinal reflexes and then transcardially perfused using a chilled 4% paraformaldehyde (PFA) solution in phosphate buffered saline (PBS) at a pH

of 7.3-7.4. Brains were extracted and allowed to post-fix in 4% PFA overnight and then placed into a 30% sucrose solution in PBS. Following the sucrose post-fix, brain sections were taken at 50 µm, placed onto gelatin-subbed slides, and allowed to dry overnight. The brain sections were then stained using a cresyl violet protocol, a Permount coverslip was applied, and sections were imaged at 10x. Electrode placements were compared against Paxinos and Watson's Rat Brain Atlas and superimposed on a section of the atlas (**Figure 4**).

Data Analysis

The raw extracellular signal was first spike-sorted using SpyKING-Circus (Yger, 2018). The results of SpyKING-Circus were exported to the Python based manual curation GUI Phy (*https://github.com/cortex-lab/phy)*. Phy was used to manually curate each dataset allowing for the labeling of good clusters, bad clusters, multi-unit activity (MUA), and allowed for the manual merging of similar clusters. Manual curation determined good clusters and was based on waveform quality, number of spikes detected per cluster, refractory violations, and quality of each cluster's autocorrelation. After manual curation, good clusters and their corresponding spike-times were loaded into MATLAB for analysis. Analyses were loosely based from Tu et. al. (2007). Spike-times were binned at 1 second. Each neuron had a baseline calculated from 5 minutes of activity prior to each injection. Each neuron's activity was then baseline normalized for each time point. A 30-minute period following the injection was parsed apart based on the following behaviors: moving, not-moving, sleeping. The behaviors were informed by locomotor activity and an average of the power in frequency bands 1-4 Hz (Delta power). Locomotor activity was binned in 1s intervals. The animal was determined to be moving if activity during the 1 second interval was greater than 1 standard deviation above the median and less than 10 standard deviations above the median. Delta power was binned into 1s intervals and z-scored. Animals were determined to be asleep if their standardized delta power exceeded the mean plus 0.5 standardized units for that 1s interval. The not-moving behavioral state was assigned when animals were determined to be awake but not moving. The average neuronal firing rate for each behavior following each injection was compared against baseline. The median of all neurons' deviation from baseline within those respective behavioral epochs was then calculated in order to find the overall change from baseline of the population of neurons per animal. Following this initial analysis, a waveform classification algorithm (Ardid, 2015) was used to determine neuron

subtypes based on whether they had a broad waveform shape (corresponding to pyramidal neurons) or a narrow waveform shape (corresponding to interneurons). The previously described baseline analysis was repeated after these neurons were parsed into broad and narrow categories. **Figure 3** describes the timeline of experimental days as well as the timepoints analyzed.

Data was checked for normality using a Kolmogorov-Smirnov test against the normal distribution except for distributions with less than 30 samples where a Shapiro-Wilk test was employed (i.e. BEC data). Firing rate distributions in all treatments and behavioral conditions were non-normally distributed. Given that not all animals fell asleep, incomplete measurements existed within the dataset which disallowed usage of non-parametric tests of repeated measures such as Friedman's Chi-Squared. Because of this, data with three or more distributions were first analyzed using the Kruskal-Wallis omnibus test. Significant omnibus tests were followed using Neymeni's test for multiple comparisons. In situations where 2 distributions were compared, the Wilcoxon's Rank-Sum test was utilized.

RESULTS

Blood Ethanol Concentration Curve

A BEC curve was generated from the data collected in the first half of the study. Awake-behaving animals received either a 1.0 g/kg or 2.0 g/kg of EtOH and had their blood drawn at the 5-, 15-, 30-, 60- and 90-minute timepoints. Mean BECs at each of the above timepoints for 1.0 g/kg are as follows: 65, 73, 76, 72, 54 mg/dL. Mean BECs at each of the above timepoints for 2.0 g/kg are as follows: 122, 151, 158, 168, 160 mg/dL. Raw data and SEM can be found in **Table 1**. Overall, IP injected EtOH exhibits dose dependent variability. This can be attributed to differences in rodent weight, intraperitoneal space, and metabolism. Additionally, the large volumes required for IP injected EtOH (2-3 mL for 1.0 g/kg, 4-6 mL for 2.0 g/kg) may play a role in the variability. A BEC curve for anesthetized animals was also collected during this study, however, differences in thermoregulation under anesthesia may lead to the tail vein being an unreliable source for BEC collection. The result of this are values significantly lower than the awake-behaving data described above and can also be found in **Table 1** and **Figure 5.**

Despite the variability exhibited, a BEC curve was reliably fit to each dose of EtOH. The theoretical BEC curve superimposed over the mean BECs above can be found in **Figure 5.** **Equation 1** depicts the nonlinear function fit to our interpolated empirical data.

$$Bec(t) = \left(1 + \ln\left(Be(t)^2\right) * p_1\right) + (1 + \ln\left(t^2 + B(t)\right) + (-p_2 * t + Bd(t)) \qquad \textbf{(1)}$$

Where Bec(t) is the BEC at time t, Be(t) is the exponential growth rate of the BEC at time t, B(t) is the parabolic growth rate of the BEC at time t, and Bd(t) is the linear decay of the BEC at time t. p_1, p_2, and are all free parameters fit to the data using default fitnlm settings in MATLAB's Optimization Toolbox (MATLAB – MA). The theoretical curve significantly predicts EtOH metabolism at both 1 g/kg ($r^2 = 0.509$, $F = 278$, $p < 0.001$) and 2 g/kg ($r^2 = 0.47$, $F = 220$, $p < 0.001$). BECs from electrophysiology experiments were not significantly different from curve predicted values at 120 minutes (One sample t-test, 1 g/kg EtOH: $t(7) = 1.5$, $p = 0.17$, 2 g/kg EtOH: $t(8) = -0.26$, $p = 0.80$). This indicates our modeled curve is a good estimate of BECs throughout the electrophysiology experiments' recording period. Data represented in mean + SEM.

Baseline Analysis of all Neurons

A baseline distribution of activity for each injection was calculated by finding the median firing rates of all neurons over a 5-minute time interval prior to each respective injection. This resulted in values for each animal's recorded neural population by which each treatment condition (saline, EtOH) would be compared. Data compared against each respective baseline was taken from the 30-minute period after each injection. Sections of time were labeled according to the behavior of the animal at each timepoint. Locomotor data and local field potential data (LFP) informed us whether the animal was awake and moving, awake and not moving, and sleeping. Distributions for each treatment condition and behavioral state were then extracted. This allowed for a finer analysis to be done on EtOH's impact on mPFC neural activity. **Figure 3** represents the time-points parsed for the analysis while **Figure 6** represents the different behavioral states' impact on firing rates while EtOH is present in the system. Ultimately each experimental group had a distribution of baseline corrected firing rates per neuron per treatment and per behavioral state.

The first experimental group received two injections of saline volume matched to a 1.0 g/kg injection of EtOH to control for the impact repeated injections may have on neural activity. The data from this group indicated a significant difference across treatment or behavior (Kruskal-Wallis: $X^2 = 26.08$, $p < 0.0001$, **Figure 7**). The significant Kruskal-Wallis test was followed up with a Nemanyi test for multiple comparisons. We found that the moving behavioral condition was significantly greater after the second saline injection in comparison to the two non-moving conditions. This suggests that gross neural activity is altered during different states of vigilance.

The second experimental group received one volume matched injection of saline followed 30 minutes later by an injection of EtOH at 1.0 g/kg. Overall there was a significant difference across groups (Kruskal-Wallis: $X^2 = 50.32$, $p < 0.0001$, **Figure 8**). Nemanyi's test for multiple comparisons found that after animals received EtOH and fell asleep, neural activity was reduced in comparison to the Saline & Moving condition as well as the EtOH & Moving condition. Importantly, neural activity in the EtOH & Sleep condition was significantly less than the Saline & Sleep condition. Last, the EtOH & Moving condition saw significantly more neural activity in comparison to the Saline & Not Moving conditions. Given that the only decrease was

seen in the EtOH & Sleep condition, it is likely that EtOH at 1.0 g/kg is modulating gross neural activity only in lowered states of vigilance such as sleep.

The last experimental group received one volume matched injection of saline followed 30 minutes later by EtOH at 2.0 g/kg. Overall there was a significant difference across groups (Kruskal-Wallis: $X^2 = 181.46$, $p < 0.0001$, **Figure 9**). The Kruskal-Wallis omnibus test was followed up with a Nemenyi's test for multiple comparisons. This revealed a significant decrease in gross neural activity in the EtOH & Sleeping condition compared with Saline & Moving, Saline & Not Moving, Saline & Sleep, EtOH & Moving, and EtOH & Not Moving conditions. Gross neural activity in the EtOH & Not Moving condition was also significantly less than the Saline & Moving condition. These results suggest that sleep and vigilance state have a major modulatory role in EtOH's impact on mPFC neural activity for the 2g/kg dose. Evidence for this is the between-treatment comparison of EtOH & Moving and EtOH & Sleep being significantly different as well as EtOH & Moving having no significant difference between all saline treatment groups.

Analysis of Behavioral State in Comparison to Anesthetized States

Unclassified neurons were grouped according to behavior state (moving, not moving, sleep) and compared against unclassified anesthetized data (see **Figure 10**). All behavioral states had a significant main effect when compared against the anesthetized data. (Kruskal-Wallis: **Moving:** $X^2 = 26.17$, $p < 0.0001$, **Not Moving:** $X^2 = 17.89$, $p < 0.0001$, **Sleep:** $X^2 = 18.97$, $p < 0.0001$). All results were followed up with Nemenyi's test for multiple comparisons. All treatments (Saline, EtOH at 1.0 g/kg, and EtOH at 2.0 g/kg) in the moving behavioral condition were significantly greater than the anesthetized EtOH condition. In the not-moving behavioral condition, no treatments significantly differed from either. In the sleep behavioral condition, only the EtOH at 2.0 g/kg treatment was significantly different than the anesthetized saline condition Therefore, in order to get decreases in firing rates similar to urethane anesthetized preparations & EtOH in awake-behaving animals - sleep and a higher dose of EtOH is necessary.

Baseline Analysis with Interneurons Separated from Pyramidal Neurons

Each neuron's waveform was utilized to classify it into either a broadly shaped pyramidal neuron or a narrow interneuron. Neurons that fit neither category were considered "in-between" by our waveform classification algorithm and discarded. A maximum of 4000 waveforms were extracted from each neuron found. A mean waveform was calculated for each neuron and then classified using a waveform classification algorithm (Ardid 2015). In order to produce a sufficient sample for the waveform classification algorithm, neurons were collapsed across group resulting in a distribution of neurons for awake-behaving recordings and a distribution of neurons for the anesthetized recordings. Both the awake-behaving (Hartigan's Dip Test: $p < 0.001$) and anesthetized (Hartigan's Dip Test: $p = 0.0023$) neurons exhibited bimodality in the first principle component. According to Ardid, 2015, this suggests the results of the classification procedure are to be believed. The results of this classification were then used to index individual neurons into broad pyramidal neurons or narrow interneurons prior to baseline analysis. A baseline analysis was then conducted as described above on the individual neural populations. The results from these analyses were largely the same as what was found without splitting the neural population.

The saline-saline treatment produced no significant difference in the interneurons (Kruskal-Wallis: $X^2 = 3.14$, $p = 0.678$) however, pyramidal neurons significantly differed (Kruskal-Wallis: $X^2 = 24.72$, $p = 0.0002$). A Nemenyi's test for multiple comparisons revealed that neural activity of pyramidal neurons in the Saline 2 & Moving condition were significantly higher than the Saline 1 and Saline 2 & NMV condition (**Figure 11**).

The saline-EtOH 1.0 g/kg treatment also had a significant difference across both interneurons (Kruskal-Wallis: $X^2 = 35.53$, $p < 0.0001$) and pyramidal neurons (Kruskal-Wallis: $X^2 = 35.33$, $p < 0.0001$). In the interneurons, Nemenyi's test for multiple comparisons revealed differences between Sal & Sleep and EtOH & NMV and EtOH & Sleep. Specifically, interneurons in the Saline & Sleep condition had significantly higher neural activity than both groups. In the pyramidal neurons, Nemenyi's test for multiple comparisons revealed differences between EtOH & Sleep and EtOH & Moving as well as Saline & Moving. Specifically, neural activity in the EtOH & Sleep condition was significantly less than both specified conditions (**Figure 12**).

The saline-EtOH 2.0 g/kg treatment resulted in a significant difference across both interneurons (Kruskal-Wallis: $X^2 = 22.66$, $p = 0.0004$) and pyramidal neurons (Kruskal-Wallis: $X^2 = 168.54$, $p < 0.0001$). Despite an overall difference in the interneuron condition, no significant differences were found after applying Nemenyi's test for multiple comparisons. In the pyramidal group, Nemenyi's test for multiple comparison revealed that the EtOH & Sleep condition saw a significant decrease in neural activity compared with all other conditions (Sal & MV, NMV, Sleep, EtOH & MV, NMV). Additionally, neural activity the EtOH & Not Moving condition was significantly less than the Saline & Moving condition (**Figure 13**). The results of the pyramidal group agree with what was found prior to waveform classification. This suggests that either the pyramidal neurons are mostly responsible for the effects detected previously or that the sample of interneurons is insufficient to detect a similar effect to what was found previously.

Last, the anesthetized dataset was classified into pyramidal neurons and interneurons. From there, a baseline was determined as described above. Data was similarly pulled from the 30 minutes after saline or the 30 minutes after EtOH at 1.0 g/kg. There was a significant main effect across all neuron types and treatments (Kruskal-Wallis: $X^2 = 134.42$, $p < 0.0001$, **Figure 14**). A Nemenyi's test for multiple comparisons was used to follow up on the Kruskal-Wallis omnibus and found that there was a significant decrease between the pyramidal neurons after EtOH and all other conditions (Saline & Pyramidal Neurons, Saline & Interneurons, EtOH & Interneurons). Interestingly, the activity of interneurons was not decreased compared to saline conditions. This may be due to the heterogeneity of interneurons in mPFC. Overall these results show a replication of previous findings where a pharmacologically relevant EtOH dose produced a significant decrease in firing rates while the animal was under urethane anesthesia (Tu, et. al. 2007).

DISCUSSION

Summary

The present experiments were conducted in order to determine whether EtOH has the same impact on the neural activity of the mPFC in awake-behaving animals as it does in anesthetized animals. We hypothesized that doses sufficient to reduce neural activity in anesthetized animals would not be sufficient to reduce neural activity in awake-behaving animals. Specifically, we believed that the 1.0 g/kg dose of EtOH would not produce any reductions in neural activity whereas doses of 2.0 g/kg of EtOH would produce modest decreases in mPFC neural activity that would be inconsistent with anesthetized animals. What we found confirmed our initial hypothesis: there is no evidence to suggest mPFC neural activity is decreased in response to EtOH in awake-behaving animals. Neither doses of 1.0 g/kg or 2.0 g/kg were sufficient to produce decreases in mPFC neural activity while the animal was awake-behaving and moving. However, decreases in activity following EtOH were found while the animal was asleep in both the 1.0 g/kg EtOH and 2.0 g/kg EtOH condition. Additionally, Further analyses indicated that in order to decrease neural activity by a magnitude similar to our urethane anesthetized animals, a higher dose of EtOH (2.0 g/kg) and sleep was required. Last, there were no major deviations from the analyses described above after classifying the recorded population of neurons into pyramidal neurons or interneurons.

The awake-behaving saline-saline condition indicated that the Saline 2 & Moving condition was greater than both the Saline 1 & Saline 2 NMV condition. This suggests that the experimental parameters and procedures used may cause innate decreases of neural activity in states of NMV that are not related to the pharmacological effects of EtOH. The awake-behaving saline-EtOH at 1.0 g/kg condition produced a significant main effect and multiple comparisons testing indicated a significant decrease in the EtOH & Sleep condition while EtOH & Moving was significantly higher than Saline & NMV further suggesting that the NMV condition may have innate decreases in neural activity unrelated to EtOH pharmacology at the 1.0 g/kg dose. In the Saline-EtOH at 2.0 g/kg condition, neural activity in the EtOH & Sleep condition was significantly reduced in comparison to all other state and treatment combinations (Saline & Moving, NMV, Sleep; EtOH & MV, NMV). Additionally, EtOH at 2.0 g/kg in the non-moving

behavioral state was also significantly lower than the Saline & Moving condition. Of additional interest is the significant difference between the sleep and movement behavioral states of EtOH at 2.0 g/kg. Given this difference and the fact that the EtOH at 2.0 g/kg movement state was not significantly different than the saline movement state, it suggests that EtOH will only decrease mPFC neural activity while the animal is in a lowered state of vigilance and has no broad effect on neural activity otherwise. This indicates that EtOH's effect on mPFC neural activity is modulated by the vigilance of the animal with neural activity in sleep-states being dose dependently decreased. Given that decision making requires a heightened state of vigilance not found in sleep, it is unlikely that a simple decrease in neural activity is responsible for EtOH's impact on cognitive processes.

Importantly, our modeled BEC curve reliably predicted BEC at the end of electrophysiological recordings. Generally, our model worked on the averaged data, however, the present analyses have yet to incorporate it given that the averaged data cannot be extrapolated to each individual animal. Introducing variables for the weight and age of the animal would make individualized BEC curves possible and further improve accuracy. Future work will incorporate biologically relevant constants for the volume of the circulator, liver, and intraperitoneal space. Unfortunately, a BEC curve for our anesthetized dataset could not be generated. This is likely due to differences in thermoregulation during urethane anesthesia leading to the tail vein being an unreliable source for BEC sampling (Korner 1968).

Other Contrasting Results Between Anesthetized and Awake-Behaving Recordings

To our knowledge, the present work is the first to look at the differential effects of EtOH on mPFC neural activity in anesthetized versus awake-behaving conditions. What we found was a significant departure from what has been reported previously in anesthetized *in vivo* recordings and *in vitro* slice preparations and will inform future studies on EtOH's acute effects on cognition. However, the present work is not the first to investigate the differences between anesthetized conditions and awake-behaving conditions in general. Several studies have shown inconsistent findings between the two experimental conditions. For example, Schonewille (2006) calls into question the biophysical property of bistability in neurons. Bistability is a property of neurons hypothesized to allow them to operate at multiple modes of firing. This phenomenon has

been widely reported in the past and has been speculated to aid in richer information propagation (Loewenstein, 2005). However, Schonewille (2006) shows that bistability is a rare occurrence in awake-behaving recordings despite being readily found in their anesthetized recordings of similar preparation. Beyond biophysical properties of neurons, sensory encoding is also affected in anesthetized conditions. Rinberg (2006) investigated the differences between encoding of odors in awake-behaving versus anesthetized mice. What they found was a more generalized response to odors in the anesthetized group and a sparse encoding of odors in the awake-behaving group. The authors concluded that the sparse code in the awake-behaving animals may have been due to neurons multiplexing for both behavioral cues and odorant cues.

Beyond the contrasts highlighted between awake-behaving and anesthetized animals above, perhaps the greatest confound of anesthetized recordings is the elimination of behavior and internal states of the animal. Goal-directed decision making is a multifaceted problem that takes into account internal states, external stimuli, and present behaviors in order to arrive at an outcome (Hasselmo, 2005; Crochet, 2019). Furthermore, behavioral states often impact the neural representations found in cortical structures (Stringer, 2019). For example, sensorimotor information about an animal's speed is integrated with visual information taken from optic flow in order to produce a more accurate representation of the mouse's movement speed in the primary visual cortex (Ayaz, 2014). Last, internal states such as hunger or thirst may greatly modulate response properties of populations of neurons (Zimmerman, 2016; Betley, 2015), and these internal states are likely not captured in anesthetized recordings. Anesthetized recordings have been critical in understanding how the brain captures sensory information, however, in understanding decision making and other higher cognitive functions, we need to thoroughly evaluate and understand populations of neurons that multiplex both sensory and behavioral representations (Krakauer, 2017).

Mechanisms of Up-Down States

At the microcircuit level, GABAergic mechanisms maintain the balance between up-down states. GABA-A receptor inhibition is necessary for most aspects of up-down states, while GABA-B receptor inhibition has a more selective role in terminating up-states of layer 2-3 cortical neurons (Crunelli, 2015). While the precise mechanism governing the switch from

typical neural function to up-down states is yet to be identified, a promising lead has come in the form of the leak potassium channel (Yoshida, 2018). The larger picture remains: a precise balance between inhibitory and excitatory mechanisms is found and maintained through GABAergic neurotransmission and this balance can be disrupted via EtOH.

At the level of neurocircuitry, it has been shown that thalamocortical circuits are necessary for the production and maintenance of up-down states. These circuits are able to precisely tune the duration and frequency of up-down states, and after silencing either the thalamus or mPFC, the probability of observing up-down states is greatly reduced (David, 2013) and the synchrony of up-down states across brain regions is lost (Lemieux, 2015). The loss of this synchrony can lead to impaired memory consolidation during sleep (Niknazar, 2015). Conversely, facilitating thalamocortical synchrony can aid in memory consolidation for those with minor cognitive impairments (Ladenbauer, 2017). In alcohol dependent patients, sleep-associated memory consolidation is significantly impaired (Junghanns, 2009). Given EtOH's role in modulating up-down states (Tu et. al., 2007), the declines seen in alcohol dependent patients' memory consolidation may be due to a loss of thalamocortical synchrony. While this can partially explain the cognitive decline associated with long-term chronic, heavy alcohol use; it cannot fully explain the acute, pharmacological actions of alcohol on cognition. However, studying the mechanisms associated with EtOH's impact on cortical up-down states may be an informative first step for understanding the mechanisms associated with awake-behaving cognitive declines in response to EtOH.

Potential Mechanisms of Acute EtOH on mPFC Mediated Behaviors

Our results indicate that there are no deficits in firing rate following EtOH at 1.0 g/kg or 2.0 g/kg while the animal is awake-behaving and a heightened state of vigilance. Yet deficits in spatial working memory have been reported as low as 0.75 g/kg. If deficits in cognition following acute EtOH are not the result of a simple decrease in neural activity, then the question remains as to how cognition is impaired following drinking. For speculation of the current results, we can turn to computational theories. The prefrontal cortex and basal ganglia (BG) model of working memory (PBWM) model suggests that the PFC operates via active maintenance of present information and rapid updating. Active maintenance is suggested to be a

phenomenon of corticocortical loops whereas rapid updating requires BG gating and corticothalamic loops. Active maintenance is mechanistically thought to be a product of recurrent excitation amongst pyramidal neurons that generate a fixed attractor point (Zipser, 1991). Rapid updating on the other hand requires BG-gating of a dopaminergic (DA) update signal. The BG operates by default on a no-go circuit to the thalamus and when rapid updating is required, a go-circuit is activated that sends a phasic dopaminergic pulse to the thalamus that then projects to the PFC in order to update the information that should be kept in active maintenance. In this way, it is acting as an amplifier of relevant signals via dopaminergic signaling (O'Reilly and Frank, 2006).

As mentioned earlier, hippocampal place cells lose spatial sensitivity in response to acute EtOH (Matthews 2002). A similar phenomenon may occur in the rodent mPFC. A mechanism to explain this phenomenon revolves around the previously mentioned PBWM model. Acute EtOH dose dependently increases DA levels in the striatum (Vena, 2016; Bannon, 1983) and mPFC (Doherty, 2016; Schier, 2013). The effect of this pharmacologically mediated increase in DA may lead to increased go-signals from the BG to the thalamus, which then would lead to persistent rapid updating in the mPFC and dysregulation of the corticothalamic and corticostriatal circuits necessary for learning and memory (Nakayama, 2018). Evidence of EtOH mediated dysregulation of corticothalamic circuits has been described above (David, 2013; Lemieux 2015) and lends well to the mentioned hypothesis. In addition, the PBWM model necessitates a trace signal in order to encode information during active maintenance and learning involving trace conditioning has been shown to be especially impaired following acute EtOH pretreatment (Hunt et. al., 2009). Conversely, facilitating mPFC activity has been shown to improve rodent learning in delayed contexts (Volle, 2016). In sum, mPFC activity would be non-specifically activated by background sensory stimuli and internal states that are otherwise ignored during decision making and working memory tasks due to persistent rapid updating caused by heightened BG DA levels. Furthermore, information that is able to be kept in working memory would require higher levels of effort for active maintenance. In other words, the noise becomes signal and the signal more quickly fades away.

Conclusions and Future Directions

In summary, we found no effect of EtOH on gross neural activity while animals were awake, behaving, and moving. Any reductions in firing rates found were during states of reduced vigilance in the animal and at the highest dose utilized in the present experiment. This contrasts to what has been found in anesthetized *in vivo* recordings where the presence of urethane and up-down states produced confounded results that showed drastic reductions in gross neural activity. EtOH seems to exert the majority of its effects on lowered states of vigilance. This suggests a conserved mechanism for the reduction of gross neural activity in both anesthetized states and sleep states. This may provide an explanation for the chronic effects of EtOH use on aspects of cognition, however, it does not provide an explanation for the acute pharmacological effects EtOH has on reduced cognitive performance. Given the present results, finding the neural correlates related to acute EtOH's impact on cognition will require more than gross-level measurements and analyses of neural activity.

Further research must leverage sophisticated behavioral measurements and cognitive tasks with state-of-the-art extracellular recording techniques. Silicon electrodes with dense recording sites will be able to provide measures of functional connectivity amongst a population of neurons in order to see how the quality of information transmission in a recorded population is either preserved or degraded following EtOH. Additionally, cognitive tasks that leverage multiple aspects of mPFC function will be able to produce dissociable results on components such as working memory, cognitive flexibility, and rule learning.

REFERENCES

Adolphs, R., Tranel, D., Damasio, H., & Damasio, A. (1994). Impaired recognition of emotion in facial expressions following bilateral damage to the human amygdala. *Nature*. https://doi.org/10.1038/372669a0

Alexander, W. H., & Brown, J. W. (2011). Medial prefrontal cortex as an action-outcome predictor. *Nature Neuroscience*, *14*(10), 1338–1344. https://doi.org/10.1038/nn.2921

Ardid, S., Vinck, M., Kaping, D., Marquez, S., Everling, S., & Womelsdorf, T. (2015). Mapping of Functionally Characterized Cell Classes onto Canonical Circuit Operations in Primate Prefrontal Cortex. *Journal of Neuroscience*, *35*(7), 2975–2991. https://doi.org/10.1523/jneurosci.2700-14.2015

Ayaz A, Saleem AB, Scholvinck ML, Carandini M: Locomotion controls spatial integration in mouse visual cortex. Curr Biol 2013, 23:890-894.

Balleine, B. W., & Dickinson, A. (1998). Goal-directed instrumental action: Contingency and incentive learning and their cortical substrates. Neuropharmacology, 37(4–5), 407–419. https://doi.org/10.1016/S0028-3908(98)00033-1

Bannon, M. J., & Roth, R. H. (1983). Pharmacology of mesocortical dopamine neurons. Pharmacological Reviews, 35(1), 53 LP – 68. Retrieved from http://pharmrev.aspetjournals.org/content/35/1/53.abstract

Bechara, A. (2005). Decision making, impulse control and loss of willpower to resist drugs: A neurocognitive perspective. *Nature Neuroscience*, *8*(11), 1458–1463. https://doi.org/10.1038/nn1584

Bechara, A., Damasio, A. R., Damasio, H., & Anderson, S. W. (1994). Insensitivity to future consequences following damage to human prefrontal cortex. *Cognition*. Netherlands: Elsevier Science. https://doi.org/10.1016/0010-0277(94)90018-3

Berendse, H. W., Graaf, Y. G., & Groenewegen, H. J. (1992). Topographical Organization and Relationship With Ventral Striatal Compartments of Prefrontal Corticostriatal Projections in the Rat, *347*, 314–347.

Betley, J. N., Xu, S., Cao, Z. F. H., Gong, R., Magnus, C. J., Yu, Y., & Sternson, S. M. (2015). Neurons for hunger and thirst transmit a negative-valence teaching signal. *Nature*, *521*(7551), 180–185. https://doi.org/10.1038/nature14416

Boudewijns, Z. S. R. M., Groen, M. R., Lodder, B., Mcmaster, M. T. B., Kalogreades, L., Haan, R. De, … Kock, J. De. (2013). Layer-specific high-frequency action potential spiking in the prefrontal cortex of awake rats, 7(June), 1–10. https://doi.org/10.3389/fncel.2013.00099

Boulouard, M., Lelong, V., Daoust, M., & Naassila, M. (2002). Chronic ethanol consumption induces tolerance to the spatial memory impairing effects of acute ethanol administration in rats. *Behavioural Brain Research*, *136*(1), 239–246. https://doi.org/10.1016/S0166-4328(02)00134-1

Breysse, E., Pelloux, Y., & Baunez, C. (2015). The Good and Bad Differentially Encoded within the Subthalamic Nucleus in Rats, *2*(October), 1–17.

Chin, V. S., Van Skike, C. E., Berry, R. B., Kirk, R. E., Diaz-Granados, J., & Matthews, D. B. (2011). Effect of acute ethanol and acute allopregnanolone on spatial memory in adolescent and adult rats. *Alcohol*, *45*(5), 473–483. https://doi.org/10.1016/j.alcohol.2011.03.001

Crochet, S., Lee, S. H., & Petersen, C. C. H. (2019). Neural Circuits for Goal-Directed Sensorimotor Transformations. Trends in Neurosciences, 42(1), 66–77. https://doi.org/10.1016/j.tins.2018.08.011

Crunelli, V., David, F., Lorincz, M. L., & Hughes, S. W. (2015). The thalamocortical network as a single slow wave-generating unit. *Current Opinion in Neurobiology*, *31*, 72–80. https://doi.org/10.1016/j.conb.2014.09.001

Cyders, M. A., Dzemidzic, M., Eiler, W. J., Coskunpinar, A., Karyadi, K., & Kareken, D. A. (2014). Negative Urgency and Ventromedial Prefrontal Cortex Responses to Alcohol Cues: FMRI Evidence of Emotion-Based Impulsivity. *Alcoholism: Clinical and Experimental Research*, *38*(2), 409–417. https://doi.org/10.1111/acer.12266

D . H . HUBEL * AND T . N . WIESEL. Physiol, J. I. I. (1959). RECEPTIVE FIELDS OF SINGLE NEURONES IN THE CAT ' S STRIATE CORTEX. 574–591.

Dao Duc, K., Parutto, P., Chen, X., Epsztein, J., Konnerth, A., & Holcman, D. (2015). Synaptic dynamics and neuronal network connectivity are reflected in the distribution of times in Up states. *Frontiers in Computational Neuroscience*, *9*(July), 1–9. https://doi.org/10.3389/fncom.2015.00096

David, F., Schmiedt, J. T., Taylor, H. L., Orban, G., Giovanni, G. Di, Uebele, V. N., … Stru, E. (2013). Essential Thalamic Contribution to Slow Waves of Natural Sleep, *33*(50), 19599–19610. https://doi.org/10.1523/JNEUROSCI.3169-13.2013

Doherty, J. M., Schier, C. J., Vena, A. A., Dilly, G. A., & Rueben, A. (2016). Medial Prefrontal Cortical Dopamine Responses During Operant Self-Administration of Sweetened Ethanol, *40*(8), 1662–1670. https://doi.org/10.1111/acer.13141

Euston, D. R., Gruber, A. J., & McNaughton, B. L. (2012). The Role of Medial Prefrontal Cortex in Memory and Decision Making. *Neuron*, *76*(6), 1057–1070. https://doi.org/10.1016/j.neuron.2012.12.002

Finn, P. R., Justus, A., Mazas, C., & Steinmetz, J. E. (1999). Working memory , executive processes and the effects of alcohol on Go / No-Go learning : testing a model of behavioral regulation and impulsivity, 465–472.

Forbes, E. E., Rodriguez, E. E., Musselman, S., & Narendran, R. (2014). Prefrontal response and frontostriatal functional connectivity to monetary reward in abstinent alcohol-dependent young adults. *PLoS ONE*, *9*(5), 1–12. https://doi.org/10.1371/journal.pone.0094640

Franzen, E. A., & Myers, R. E. (1973). Neural control of social behavior: Prefrontal and anterior temporal cortex. *Neuropsychologia*, *11*(2), 141–157. https://doi.org/10.1016/0028-3932(73)90002-X

García-Moreno, L. M., & Cimadevilla, J. M. (2012). Acute and chronic ethanol intake: Effects on spatial and non-spatial memory in rats. *Alcohol*, *46*(8), 757–762. https://doi.org/10.1016/j.alcohol.2012.08.001

Gentry, R. N., & Roesch, M. R. (2018). Neural activity in ventral medial prefrontal cortex is modulated more before approach than avoidance during reinforced and extinction trial blocks. *The Journal of Neuroscience*, *38*(19), 2579–17. https://doi.org/10.1523/JNEUROSCI.2579-17.2018

Givens, B. (1995). Low Doses of Ethanol Impair Spatial Working Memory and Reduce Hippocampal Theta Activity. *Alcoholism: Clinical and Experimental Research*, *19*(3), 763–767. https://doi.org/10.1111/j.1530-0277.1995.tb01580.x

Gretenkord, S., Rees, X. A., Whittington, M. A., Gartside, S. E., & Lebeau, F. E. N. (2019). Dorsal vs . ventral differences in fast Up-state-associated oscillations in the medial prefrontal cortex of the urethane-anesthetized rat, 1126–1142. https://doi.org/10.1152/jn.00762.2016

Gulick, D., & Gould, T. J. (2007). Acute ethanol has biphasic effects on short- and long-term memory in both foreground and background contextual fear conditioning in C57BL/6 mice. Alcoholism: Clinical and Experimental Research, 31(9), 1528–1537. https://doi.org/10.1111/j.1530-0277.2007.00458.x

Gundersen, H., Specht, K., Grüner, R., Ersland, L., & Hugdahl, K. (2008). Separating the effects of alcohol and expectancy on brain activation: An fMRI working memory study. *NeuroImage*, *42*(4), 1587–1596. https://doi.org/10.1016/j.neuroimage.2008.05.037

Gutman, A. L., Nett, K. E., Cosme, C. V., Worth, W. R., Gupta, S. C., Wemmie, J. A., & LaLumiere, R. T. (2017). Extinction of Cocaine Seeking Requires a Window of Infralimbic Pyramidal Neuron Activity after Unreinforced Lever Presses. *The Journal of Neuroscience*, *37*(25), 6075–6086. https://doi.org/10.1523/JNEUROSCI.3821-16.2017

Hara, K., & Harris, R. A. (2002). The anesthetic mechanism of urethane: The effects on neurotransmitter-gated ion channels. Anesthesia and Analgesia, 94(2), 313–318. https://doi.org/10.1213/00000539-200202000-00015

Hasselmo M. E. (2005). A model of prefrontal cortical mechanisms for goal-directed behavior. *Journal of cognitive neuroscience*, *17*(7), 1115–1129. doi:10.1162/0898929054475190

Hunt, P. S., Levillain, M. E., Spector, B. M., & Kostelnik, L. A. (2009). Neurobiology of Learning and Memory Post-training ethanol disrupts trace conditioned fear in rats : Effects of timing of ethanol , dose and trace interval duration. *Neurobiology of Learning and Memory*, *91*(1), 73–80. https://doi.org/10.1016/j.nlm.2008.10.001

Jahn, A., Nee, D. E., Alexander, W. H., & Brown, J. W. (2016). Distinct Regions within Medial Prefrontal Cortex Process Pain and Cognition. *The Journal of Neuroscience*, *36*(49), 12385–12392. https://doi.org/10.1523/JNEUROSCI.2180-16.2016

Kalaska, J. F. (2019). Emerging ideas and tools to study the emergent properties of the cortical neural circuits for voluntary motor control in non-human primates [version 1 ; peer review : 4 approved], *8*, 1–13.

Ketchum, M. J., Weyand, T. G., Weed, P. F., & Winsauer, P. J. (2016). Learning by subtraction: Hippocampal activity and effects of ethanol during the acquisition and performance of response sequences. *Hippocampus*, *26*(5), 601–622. https://doi.org/10.1002/hipo.22545

Ketchum, M. J., Weyand, T. G., Weed, P. F., & Winsauer, P. J. (2016). Learning by subtraction: Hippocampal activity and effects of ethanol during the acquisition and performance of response sequences. *Hippocampus*, *26*(5), 601–622. https://doi.org/10.1002/hipo.22545

Khoo, S. Y., Sciascia, J. M., Pettorelli, A., Maddux, J.-M. N., & Chaudhri, N. (2019). The medial prefrontal cortex is required for responding to alcohol-predictive cues but only in the absence of alcohol delivery. Journal of Psychopharmacology, 33(7), 842–854. https://doi.org/10.1177/0269881119844180

Killcross, S., & Coutureau, E. (2003). Coordination of Actions and Habits in the Medial Prefrontal Cortex of Rats, *2*, 400–408.

Korner, P. I., Langsford, G., Starr, D., Uther, J. B., Ward, W., & White, S. W. (1968). The effects of chloralose-urethane and sodium pentobarbitone anaesthesia on the local and autonomic components of the circulatory response to arterial hypoxia. The Journal of physiology, 199(2), 283–302. doi:10.1113/jphysiol.1968.sp008654

Krakauer, J. W., Ghazanfar, A. A., Gomez-Marin, A., MacIver, M. A., & Poeppel, D. (2017). Neuroscience Needs Behavior: Correcting a Reductionist Bias. *Neuron*, *93*(3), 480–490. https://doi.org/10.1016/j.neuron.2016.12.041

Kutlu, M. G., & Gould, T. J. (2016). Effects of drugs of abuse on hippocampal plasticity and hippocampus-dependent learning and memory: contributions to development and maintenance of addiction. *Learning & Memory*, *23*(10), 515–533. https://doi.org/10.1101/lm.042192.116

Ladenbauer, X. J., Ladenbauer, X. J., Ku, N., Boor, R. De, Avramova, E., Grittner, X. U., … Theory, N. (2017). Promoting Sleep Oscillations and Their Functional Coupling by Transcranial Stimulation Enhances Memory Consolidation in Mild Cognitive Impairment, *37*(30), 7111–7124. https://doi.org/10.1523/JNEUROSCI.0260-17.2017

Lemieux, M., Chauvette, S., & Timofeev, I. (2015). Neocortical inhibitory activities and long-range afferents contribute to the synchronous onset of silent states of the neocortical slow oscillation. *Journal of Neurophysiology*, *113*(3), 768–779. https://doi.org/10.1152/jn.00858.2013

Linsenbardt, D. N., & Lapish, C. C. (2015). Neural Firing in the Prefrontal Cortex During Alcohol Intake in Alcohol-Preferring "P" Versus Wistar Rats. *Alcoholism: Clinical and Experimental Research*, *39*(9), 1642–1653. https://doi.org/10.1111/acer.12804

Linsenbardt, D. N., Timme, N. M., & Lapish, C. C. (2019). Encoding of the Intent to Drink Alcohol by the Prefrontal Cortex is blunted in Rats with a Family History of Excessive Drinking. *Eneuro*, ENEURO.0489-18.2019. https://doi.org/10.1523/ENEURO.0489-18.2019

Livy, D. J., Parnell, S. E., & West, J. R. (2003). Blood ethanol concentration profiles: A comparison between rats and mice. Alcohol, 29(3), 165–171. https://doi.org/10.1016/S0741-8329(03)00025-9

Loewenstein, Y., Mahon, S., Chadderton, P., Kitamura, K., Sompolinsky, H., Yarom, Y., & Häusser, M. (2005). Bistability of cerebellar Purkinje cells modulated by sensory stimulation, *8*(2), 202–211. https://doi.org/10.1038/nn1393

Lovinger, D. M., White, G., & Weight, F. F. (1990). Ethanol inhibition of neuronal glutamate receptor function. *Ann Med*, *22*(4), 247–252. https://doi.org/10.3109/07853899009148935

Malagon-Vina, H., Ciocchi, S., Passecker, J., Dorffner, G., & Klausberger, T. (2018). Fluid network dynamics in the prefrontal cortex during multiple strategy switching. *Nature Communications*, *9*(1), 1–13. https://doi.org/10.1038/s41467-017-02764-x

Marinkovic, K., Rickenbacher, E., Azma, S., & Artsy, E. (2012). Acute alcohol intoxication impairs top-down regulation of stroop incongruity as revealed by blood oxygen level-dependent functional magnetic resonance imaging. *Human Brain Mapping*, *33*(2), 319–333. https://doi.org/10.1002/hbm.21213

Marszalek-grabska, M., Gibula-bruzda, E., Bodzon-kulakowska, A., Suder, P., & Gawel, K. (2018). Effects of the Positive Allosteric Modulator of Metabotropic Glutamate Receptor 5 , VU-29 , on Impairment of Novel Object Recognition Induced by Acute Ethanol and Ethanol Withdrawal in Rats, 607–620.

Matthews, D. B., & Morrow, a L. (2000). Function in the Rat, *130*, 122–130.

Matthews, D. B., Sirnson, P. E., & Best, P. J. (2002). Ethanol Alters Spatial Processing of Hippocampal Place Cells : A Mechanism for Impaired Navigation When Intoxicated, *20*(2), 404–407.

Mishra, D., Harrison, N. R., Gonzales, C. B., Schilström, B., & Konradsson-Geuken, Å. (2015). Effects of age and acute ethanol on glutamatergic neurotransmission in the medial prefrontal cortex of freely moving rats using enzyme-based microelectrode amperometry. *PLoS ONE*, *10*(4), 1–15. https://doi.org/10.1371/journal.pone.0125567

Moorman, D. E., & Aston-Jones, G. (2015). Prefrontal neurons encode context-based response execution and inhibition in reward seeking and extinction. *Proceedings of the National Academy of Sciences*, *112*(30), 9472–9477. https://doi.org/10.1073/pnas.1507611112

Moorman, D. E., James, M. H., Mcglinchey, E. M., & Aston-jones, G. (2015). Differential roles of medial prefrontal subregions in the regulation of drug seeking. *Brain Research*, *1628*, 130–146. https://doi.org/10.1016/j.brainres.2014.12.024

Morgan, M. A., & Ledoux, J. E. (1995). Differential Contribution of Dorsal and Ventral Medial Prefrontal Cortex to the Acquisition and Extinction of Conditioned Fear in Rats, *109*(4), 681–688.

Niknazar, M., Krishnan, G. P., Bazhenov, M., & Mednick, S. C. (2015). Coupling of Thalamocortical Sleep Oscillations Are Important for Memory Consolidation in Humans, 1–14. https://doi.org/10.1371/journal.pone.0144720

Nimitvilai, S., Lopez, M. F., Mulholland, P. J., & Woodward, J. J. (2016). Chronic Intermittent Ethanol Exposure Enhances the Excitability and Synaptic Plasticity of Lateral Orbitofrontal Cortex Neurons and Induces a Tolerance to the Acute Inhibitory Actions of Ethanol. *Neuropsychopharmacology*, *41*(4), 1112–1127. https://doi.org/10.1038/npp.2015.250

Onos, K. D., Francoeur, M. J., Wormwood, B. A., Miller, R. L. A., Gibson, B. M., & Mair, R. G. (2016). Prefrontal neurons encode actions and outcomes in conjunction with spatial location in rats performing a dynamic delayed non-Match to position task. *PLoS ONE*, *11*(2), 1–23. https://doi.org/10.1371/journal.pone.0149019

Pezze, M. A., Marshall, H. J., Fone, K. C. F., & Cassaday, H. J. (2015). Dopamine D 1 receptor stimulation modulates the formation and retrieval of novel object recognition memory : Role of the prelimbic cortex. *European Neuropsychopharmacology*, *25*(11), 2145–2156. https://doi.org/10.1016/j.euroneuro.2015.07.018

Popke, E. J., Allen, S. R., & Paule, M. G. (2000). Effects of acute ethanol on indices of cognitive-behavioral performance in rats. *Alcohol*, *20*(2), 187–192. https://doi.org/10.1016/S0741-8329(99)00081-6

Quiquempoix, M., Fayad, S. L., Boutourlinsky, K., Leresche, N., Lambert, C., & Bessaih, T. (2018). Layer 2 / 3 Pyramidal Neurons Control the Gain of Cortical Output. https://doi.org/10.1016/j.celrep.2018.08.038

Quiroga, R. Q., Reddy, L., Kreiman, G., Koch, C., & Fried, I. (2005). Invariant visual representation by single neurons in the human brain, *435*(June), 1102–1107. https://doi.org/10.1038/nature03687

Reilly, R. C. O. (2006). Models of High-Level Cognition, (October), 91–95.

Reilly, R. C. O., & Frank, M. J. (2006). Making Working Memory Work : A Computational Model of Learning in the Prefrontal Cortex and Basal Ganglia, *328*, 283–328.

Riaz, S., Puveendrakumaran, P., Khan, D., Yoon, S., Hamel, L., & Ito, R. (2019). Prelimbic and infralimbic cortical inactivations attenuate contextually driven discriminative responding for reward, (August 2018), 1–13. https://doi.org/10.1038/s41598-019-40532-7

Rinberg, D., Koulakov, A., & Gelperin, A. (2006). Sparse Odor Coding in Awake Behaving Mice, *26*(34), 8857–8865. https://doi.org/10.1523/JNEUROSCI.0884-06.2006

Rogers, J., Siggins, G. R., Schulman, J. A., & Bloom, F. E. (1980). Electrophysiology, *196*, 183–198.

Rothschild, G., Eban, E., & Frank, L. M. (2017). A cortical-hippocampal-cortical loop of information processing during memory consolidation. *Nature Neuroscience*, *20*(2), 251–259. https://doi.org/10.1038/nn.4457

Ryabinin, A. E., Miller, M. N., & Durrant, S. (2002). Effects of acute alcohol administration on object recognition learning in C57BL / 6J mice, *71*, 307–312.

Saddoris, M. P., & Carelli, R. M. (2014). Cocaine Self-Administration Abolishes Associative Neural Encoding in the Nucleus Accumbens Necessary for Higher-Order Learning. *Biological Psychiatry*, *75*(2), 156–164. https://doi.org/10.1016/j.biopsych.2013.07.037

Sanchez-Vives, M. V., Mattia, M., Compte, A., Perez-Zabalza, M., Winograd, M., Descalzo, V. F., & Reig, R. (2010). Inhibitory Modulation of Cortical Up States. *Journal of Neurophysiology*, *104*(3), 1314–1324. https://doi.org/10.1152/jn.00178.2010

Saults, J. S., Cowan, N., Sher, K. J., & Moreno, M. V. (2007). Differential effects of alcohol on working memory: distinguishing multiple processes. Experimental and clinical psychopharmacology, 15(6), 576–587. doi:10.1037/1064-1297.15.6.576

Saults, J. S., Cowan, N., Sher, K. J., & Moreno, M. V. (2009). NIH Public Access, *15*(6), 576–587. https://doi.org/10.1037/1064-1297.15.6.576.Differential

Saxena, S., & Cunningham, J. P. (n.d.). ScienceDirect Towards the neural population doctrine. *Current Opinion in Neurobiology*, *55*, 103–111. https://doi.org/10.1016/j.conb.2019.02.002

Schier, C. J., Dilly, G. A., & Gonzales, R. A. (2013). Intravenous Ethanol Increases Extracellular Dopamine in the Medial Prefrontal Cortex of the Long – Evans Rat, *37*(5), 740–747. https://doi.org/10.1111/acer.12042

Schonewille, M; Khosrovanl, S; Winkelman, BHJ; et al. Purkinje cells in awake behaving animals operate at the upstate membrane potential. NATURE NEUROSCIENCE Volume: 9 Issue: 4 Pages: 459-461 Published: APR 2006

Schultz, W. (1998). Predictive Reward Signal of Dopamine Neurons. *Journal of Neurophysiology*, *80*(1), 1–27. https://doi.org/10.1152/jn.1998.80.1.1

Selim, M., & Bradberry, C. W. (1996). Effect of ethanol on extracellular 5-HT and glutamate in the nucleus accumbens and prefrontal cortex: Comparison between the Lewis and Fischer 344 rat strains. *Brain Research*, *716*(1–2), 157–164. https://doi.org/10.1016/0006-8993(95)01385-7

Seo, D., Lacadie, C. M., Tuit, K., Hong, K. I., Todd Constable, R., & Sinha, R. (2013). Disrupted ventromedial prefrontal function, alcohol craving, and subsequent relapse risk. *JAMA Psychiatry*, *70*(7), 727–739. https://doi.org/10.1001/jamapsychiatry.2013.762

SIGGINS, G. R., BLOOM, F. E., FRENCH, E. D., MADAMBA, S. G., MANCILLAS, J., PITTMAN, Q. J., & ROGERS, J. (1987). Electrophysiology of Ethanol on Central Neurons. *Annals of the New York Academy of Sciences*, *492*(1), 350–366. https://doi.org/10.1111/j.1749-6632.1987.tb48692.x

Simon, H. A., & Newell, A. (1970). Human problem solving:

Skike, C. E. Van, Goodlett, C., & Matthews, D. B. (2019). Acute alcohol and cognition : Remembering what it causes us to forget. *Alcohol*, *79*, 105–125. https://doi.org/10.1016/j.alcohol.2019.03.006

Song, X. C., & Moyer, J. R. (2017). Layer- and subregion-specific differences in the neurophysiological properties of rat medial prefrontal cortex pyramidal neurons, 177–191. https://doi.org/10.1152/jn.00146.2017

Stringer, C., Pachitariu, M., Steinmetz, N., Reddy, C. B., Carandini, M., & Harris, K. D. (2019). Spontaneous behaviors drive multidimensional, brainwide activity. *Science*, *364*(6437). https://doi.org/10.1126/science.aav7893

Tamura, M., Spellman, T. J., Rosen, A. M., Gogos, J. A., & Gordon, J. A. (2017). Hippocampal-prefrontal theta-gamma coupling during performance of a spatial working memory task. *Nature Communications*, *8*(1), 2182. https://doi.org/10.1038/s41467-017-02108-9

Tang, W., Shin, J. D., Frank, L. M., & Jadhav, S. P. (2017). Hippocampal-Prefrontal Reactivation during Learning Is Stronger in Awake Compared with Sleep States. *The Journal of Neuroscience*, *37*(49), 11789–11805. https://doi.org/10.1523/JNEUROSCI.2291-17.2017

Tanimizu, T., Kono, K., & Kida, S. (2018). Brain networks activated to form object recognition memory. *Brain Research Bulletin*, *141*(May 2017), 27–34. https://doi.org/10.1016/j.brainresbull.2017.05.017

Trantham-Davidson, H., Burnett, E. J., Gass, J. T., Lopez, M. F., Mulholland, P. J., Centanni, S. W., … Chandler, L. J. (2014). Chronic Alcohol Disrupts Dopamine Receptor Activity and the Cognitive Function of the Medial Prefrontal Cortex. *Journal of Neuroscience*, *34*(10), 3706–3718. https://doi.org/10.1523/JNEUROSCI.0623-13.2014

Tu, Y., Kroener, S., Abernathy, K., Lapish, C., Seamans, J., Chandler, L. J., & Woodward, J. J. (2007). Ethanol Inhibits Persistent Activity in Prefrontal Cortical Neurons. *Journal of Neuroscience*, *27*(17), 4765–4775. https://doi.org/10.1523/JNEUROSCI.5378-06.2007

van Eden, C. G., & Uylings, H. B. M. (1985). Cytoarchitectonic development of the prefrontal cortex in the rat. Journal of Comparative Neurology, 241(3), 253–267. https://doi.org/10.1002/cne.902410302

van Gaal, S., Ridderinkhof, K. R., Fahrenfort, J. J., Scholte, H. S., & Lamme, V. A. F. (2008). Frontal Cortex Mediates Unconsciously Triggered Inhibitory Control. *Journal of Neuroscience*, *28*(32), 8053–8062. https://doi.org/10.1523/JNEUROSCI.1278-08.2008

Varodayan, F. P., Sidhu, H., Kreifeldt, M., Roberto, M., & Contet, C. (2018). Neuropharmacology Morphological and functional evidence of increased excitatory signaling in the prelimbic cortex during ethanol withdrawal. *Neuropharmacology*, *133*, 470–480. https://doi.org/10.1016/j.neuropharm.2018.02.014

Vena, A. A., Mangieri, R., & Gonzales, R. A. (2016). Regional Analysis of the Pharmacological Effects of Acute Ethanol on Extracellular Striatal Dopamine Activity, *40*(12), 2528–2536. https://doi.org/10.1111/acer.13246

Vertes, R. P. (2004). Differential projections of the infralimbic and prelimbic cortex in the rat. *Synapse*, *51*(1), 32–58. https://doi.org/10.1002/syn.10279

Vertes, R. P. (2006). INTERACTIONS AMONG THE MEDIAL PREFRONTAL CORTEX , HIPPOCAMPUS AND MIDLINE THALAMUS IN EMOTIONAL AND COGNITIVE PROCESSING IN THE RAT, *142*, 1–20. https://doi.org/10.1016/j.neuroscience.2006.06.027

Vidal-gonzalez, I., Vidal-gonzalez, B., Rauch, S. L., & Quirk, G. J. (2006). Microstimulation reveals opposing influences of prelimbic and infralimbic cortex on the expression of conditioned fear, (787), 728–733. https://doi.org/10.1101/lm.306106.728

Volle, J., Yu, X., Sun, H., Tanninen, S. E., & Insel, N. (2016). Enhancing Prefrontal Neuron Activity Enables Associative Learning of Temporally Disparate Events Article Enhancing Prefrontal Neuron Activity Enables Associative Learning of Temporally Disparate Events. *CellReports*, *15*(11), 2400–2410. https://doi.org/10.1016/j.celrep.2016.05.021

Weissenborn, R., & Duka, T. (2003). Acute alcohol effects on cognitive function in social drinkers : their relationship to drinking habits, 306–312. https://doi.org/10.1007/s00213-002-1281-1

Weitlauf, C., & Woodward, J. J. (2008). Ethanol selectively attenuates nmdar-mediated synaptic transmission in the prefrontal cortex. *Alcoholism: Clinical and Experimental Research*, *32*(4), 690–698. https://doi.org/10.1111/j.1530-0277.2008.00625.x

Whitten, T. A., Martz, L. J., Guico, A., Gervais, N., & Dickson, C. T. (2009). Heat synch: Inter- and independence of body-temperature fluctuations and brain-state alternations in urethane-anesthetized rats. Journal of Neurophysiology, 102(3), 1647–1656. https://doi.org/10.1152/jn.00374.2009

Wilhelm, C. J., & Mitchell, S. H. (2012). Acute ethanol does not always affect delay discounting in rats selected to prefer or avoid ethanol. *Alcohol and Alcoholism*, *47*(5), 518–524. https://doi.org/10.1093/alcalc/ags059

Wit, H. D. E., & Mitchell, S. H. (2009). DISCOUNTING.

Wood, D. A., Walker, T. L., & Rebec, G. V. (2011). Experience-dependent changes in neuronal processing in the nucleus accumbens shell in a discriminative learning task in differentially housed rats. *Brain Research*, *1390*, 90–98. https://doi.org/10.1016/j.brainres.2011.03.023

Wright, M. J., Vandewater, S. A., & Taffe, M. A. (2013). The influence of acute and chronic alcohol consumption on response time distribution in adolescent rhesus macaques. *Neuropharmacology*, *70*, 12–18. https://doi.org/10.1016/j.neuropharm.2013.01.003

Yger, P., Spampinato, G. L. B., Esposito, E., Lefebvre, B., Deny, S., Gardella, C., … Marre, O. (2018). A spike sorting toolbox for up to thousands of electrodes validated with ground truth recordings in vitro and in vivo. *ELife*, *7*, 1–23. https://doi.org/10.7554/eLife.34518

Yoshida, K., Shi, S., Ukai-Tadenuma, M., Fujishima, H., Ohno, R., & Ueda, H. R. (2018). Leak potassium channels regulate sleep duration. *Proceedings of the National Academy of Sciences*, *115*(40), E9459–E9468. https://doi.org/10.1073/pnas.1806486115

Zagha, E., & McCormick, D. A. (2014). Neural control of brain state. *Current Opinion in Neurobiology*, *29*(1), 178–186. https://doi.org/10.1016/j.conb.2014.09.010

Zimmerman, C. A., Lin, Y. C., Leib, D. E., Guo, L., Huey, E. L., Daly, G. E., … Knight, Z. A. (2016). Thirst neurons anticipate the homeostatic consequences of eating and drinking. *Nature*, *537*(7622), 680–684. https://doi.org/10.1038/nature18950

Zipser, D. (1991). Recurrent Network Model of the Neural Mechanism of Short-Term Active Memory, *193*, 179–193.

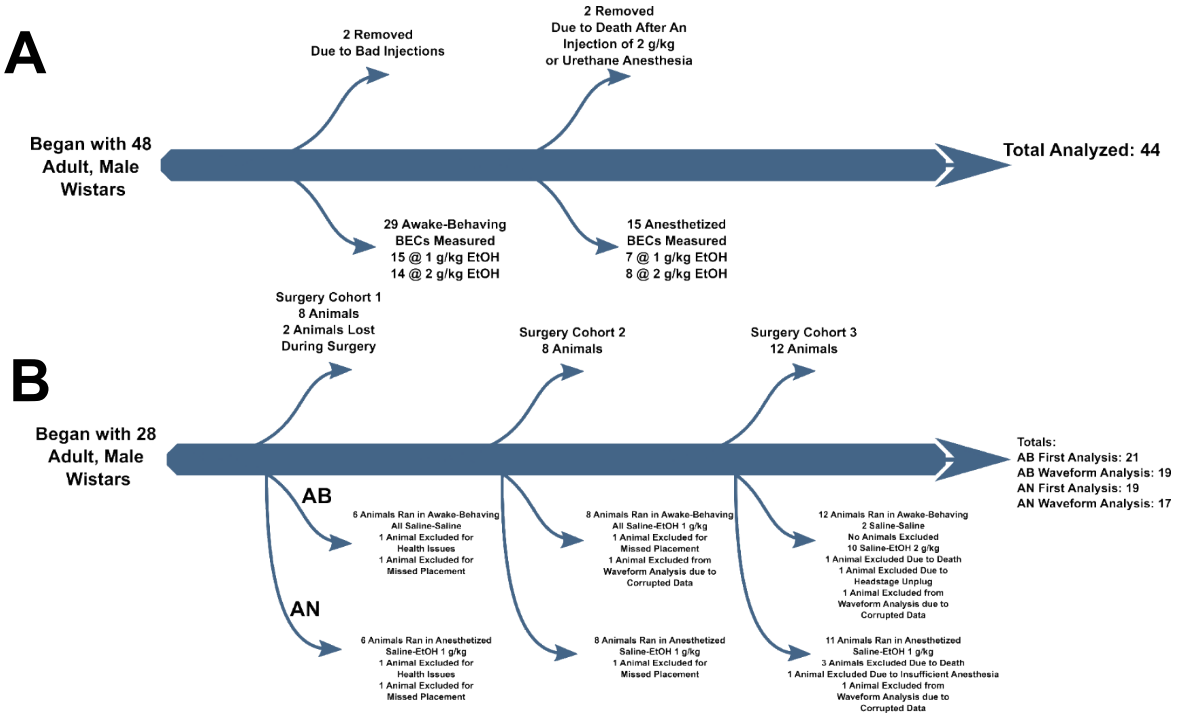

Figure 1. Description of animal use.

Description of animal totals and causes of exclusion. **A** describes animal attrition during the BEC curve experiments while **B** describes animal attrition during electrophysiology experiments. AB = awake-behaving, AN = anesthetized.

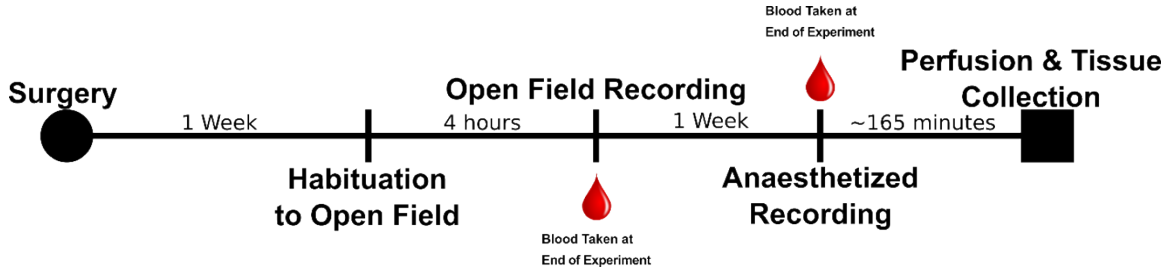

Figure 2. Experimental timeline.

Experimental timeline for all animals used in electrophysiological studies. Implantation of probe was done as described in the Methods. Animals were allowed to recover for at least 1 week. Following this, animals were habituated to the open field testing environment for 15 minutes. 4 hours after habituation, testing began. Following testing, blood was drawn to determine BECs. Animals sat for at least 1 week prior to anesthetized recordings in order to minimize any lingering effects of acute ethanol. Blood was drawn after the anesthetized recordings and all animals were then subsequently perfused and their brains were extracted.

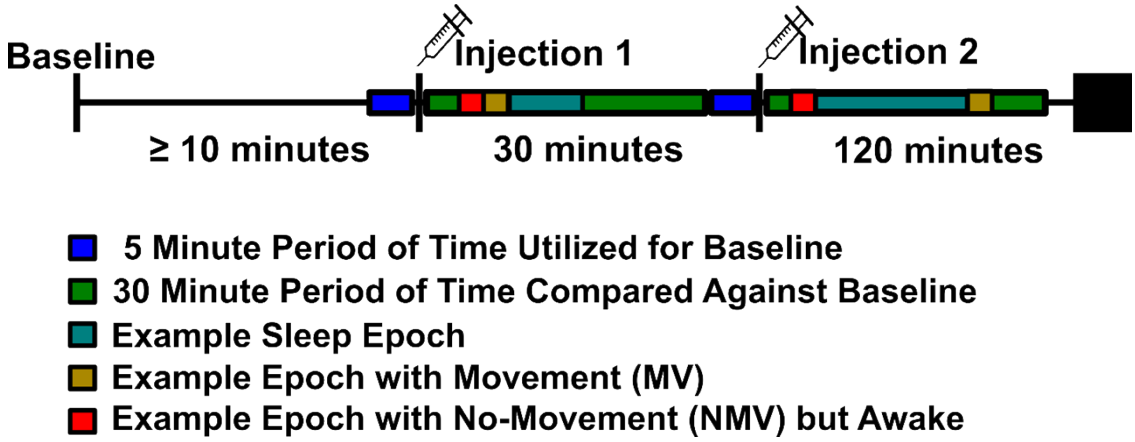

Figure 3. Recording timeline.

Test day timeline for all awake-behaving and anesthetized groups. A period of at least 10 minutes was utilized for baseline. Injection 1 took place after the baseline period and neural activity was recorded for 30 minutes afterwards. Injection 2 took place after those 30 minutes and was either saline, EtOH at 1 g/kg, or EtOH at 2 g/kg. Neural activity was recorded for at least 120 minutes after injection 2. Areas marked in blue on the timeline are representative of the 5 minute period of time prior to an injection that was utilized for baseline. Areas in green or flanked by green blocks indicate the 30 minute period of time that was included in the present analyses. For the awake-behaving recordings, animals had their behaviors parsed: blue indicates an example sleep epoch, mustard yellow indicates an example epoch with movement, and red indicates an example epoch where the animal is not moving but awake.

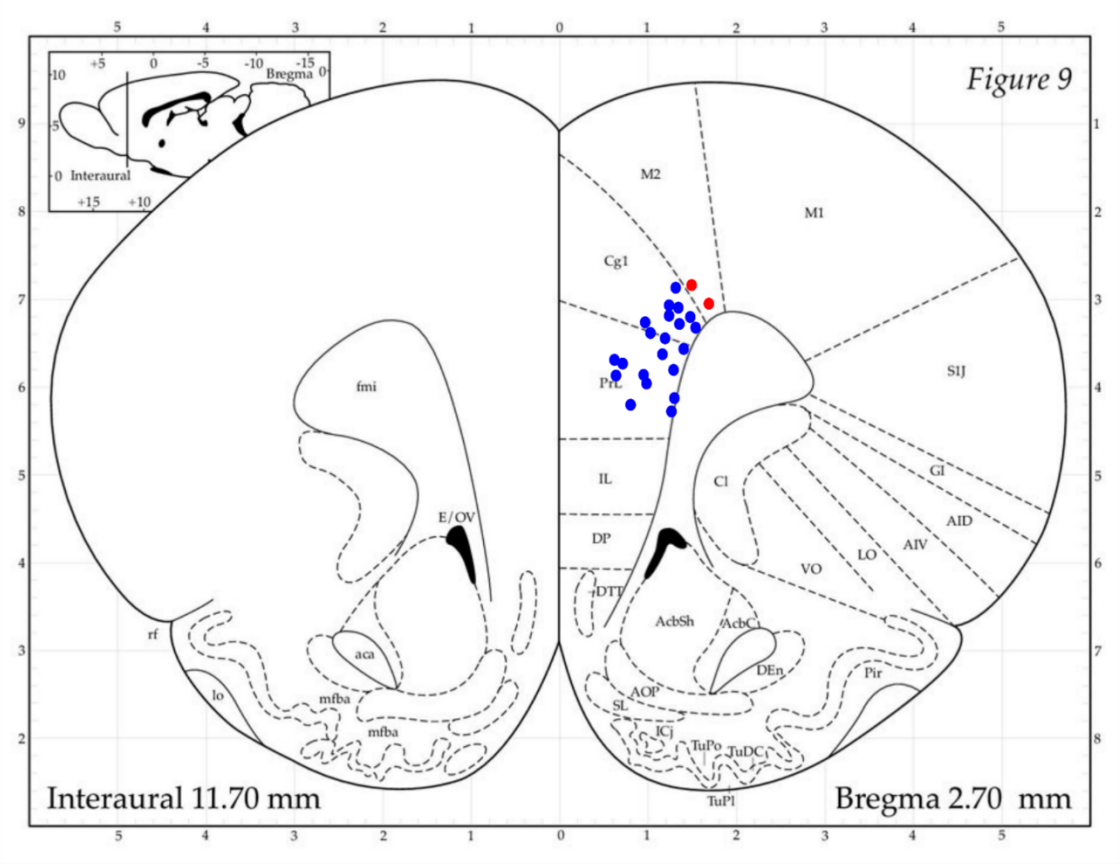

Figure 4. Histological confirmation of electrode placement.

Histological confirmation of hits and misses in electrophysiological experiments. Blue dots indicate areas included in the analysis while red dots indicate areas excluded from the analysis. All included data was within the dorsal mPFC comprising the cingulate and prelimbic subregions.

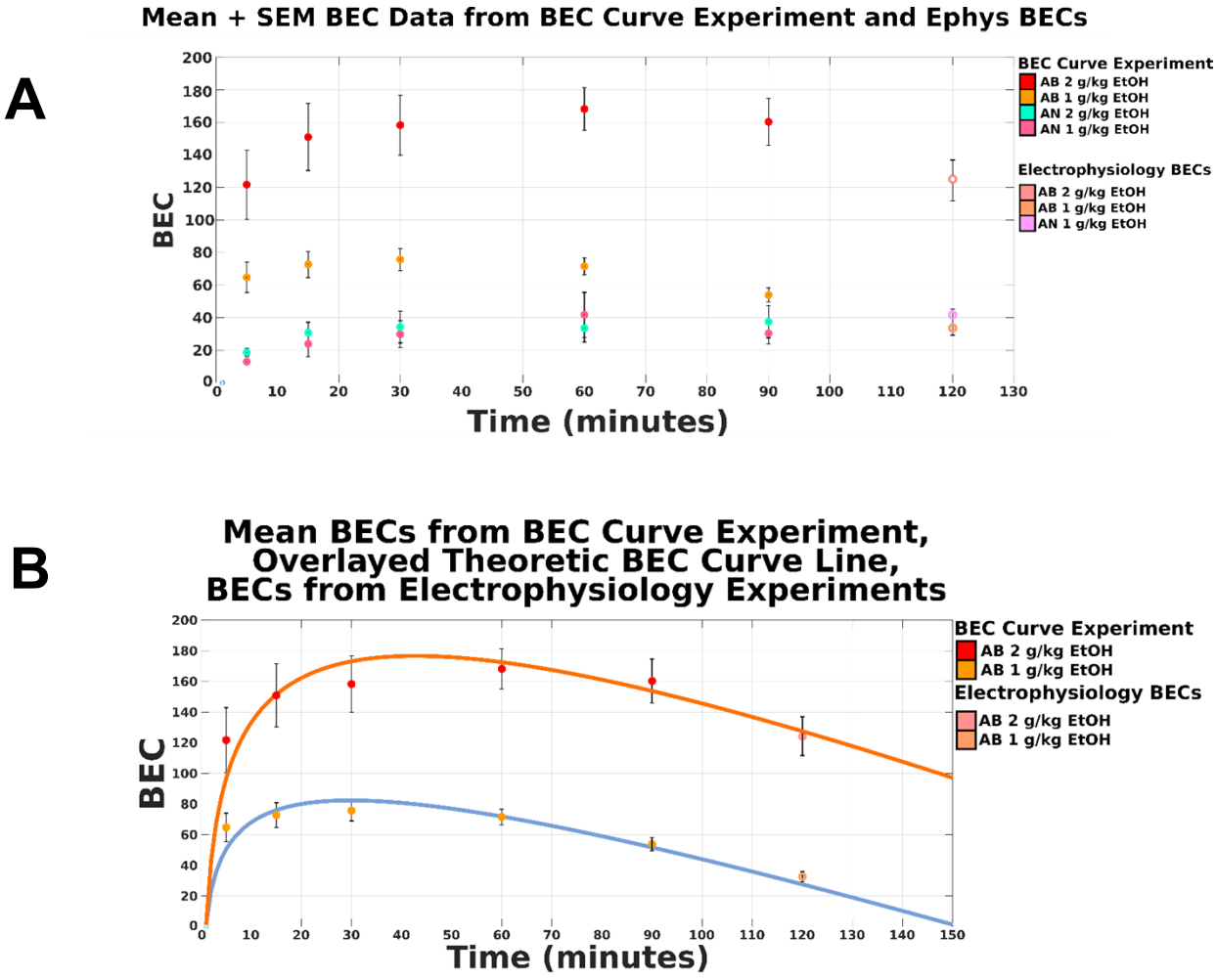

Figure 5. Blood ethanol concentration data and modeled BEC.

A. BEC curve data presented as the mean + SEM. BEC Curve experiment data includes both awake-behaving and anesthetized cohorts as well as doses of 1 g/kg and 2 g/kg of EtOH. BECs from electrophysiological experiments are also represented at minute 120. **B.** A blood ethanol concentration (BEC) curve was generated using a separate cohort of animals. The curve significantly predicts EtOH metabolism at both 1 g/kg ($r^2 = 0.509$, $F = 278$, $p < 0.001$) and 2 g/kg ($r^2 = 0.47$, $F = 220$, $p < 0.001$). BECs from electrophysiology experiments were not significantly different from curve predicted values at 120 minutes (1 g/kg EtOH: $t(7) = 1.5$, $p = 0.17$, 2 g/kg EtOH: $t(8) = -0.26$, $p = 0.80$). This indicates our modeled curve is a good estimate of BECs throughout the electrophysiology experiments' recording period. Data represented in mean + SEM.

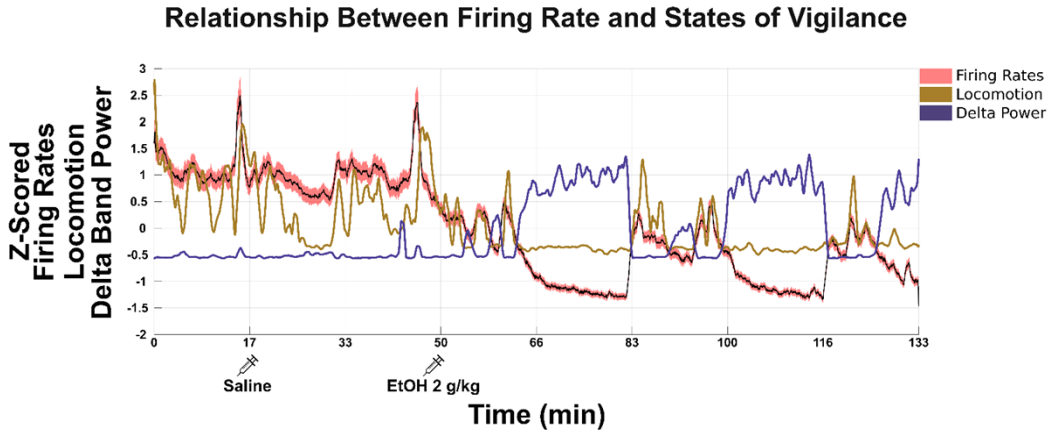

Figure 6. Representative time course describing impact of sleep and locomotion

Representative time course from an individual animal in Group 3 (Saline followed by 2 g/kg ethanol). Mean z-score over time of 33 neurons + SEM. 1 second bins.

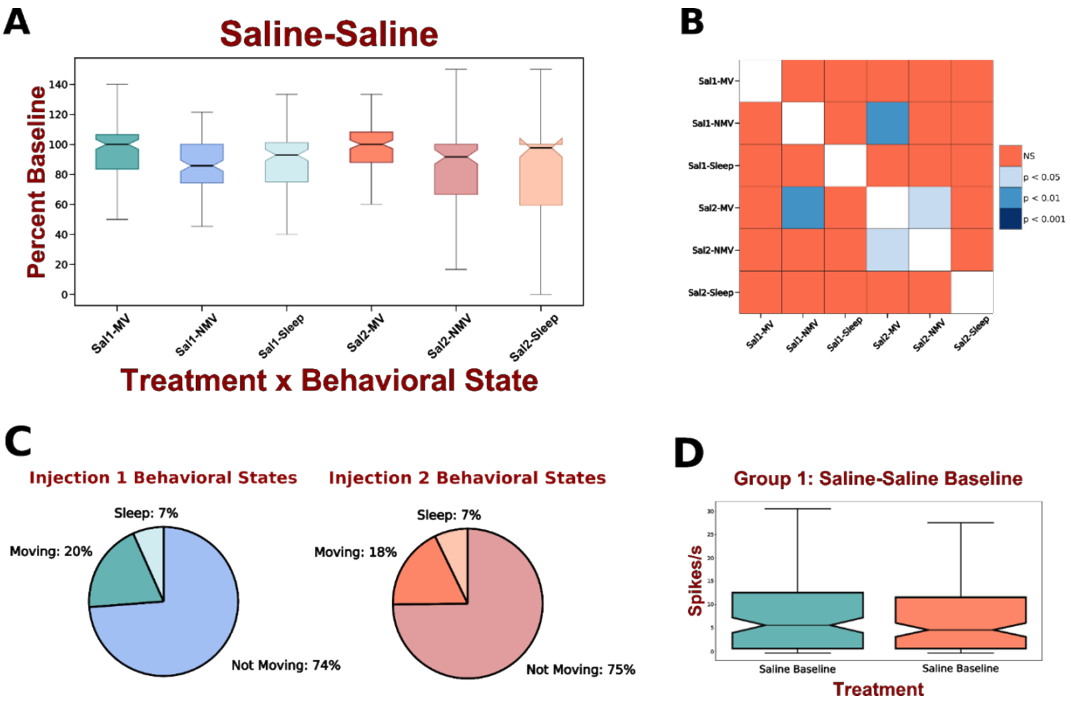

Figure 7. No gross impact of repeated saline injections.

A. Box plots indicate distribution of baseline corrected firing rates per neuron per treatment and behavioral state. **B.** A Kruskal-Wallis omnibus test ($X^2 = 26.08$, $p < 0.00001$) was followed by a Nemenyi post-hoc test. Blue shades indicate varying levels of significance. Gross firing rates in the Saline-Saline condition are reduced in non-moving states. **C**. Pie charts represent amount of time spent in each behavioral state per treatment. **D.** Comparison of baselines used to baseline normalize each treatment condition. A Wilcoxon ranked sum test indicated that baselines did not significantly differ.

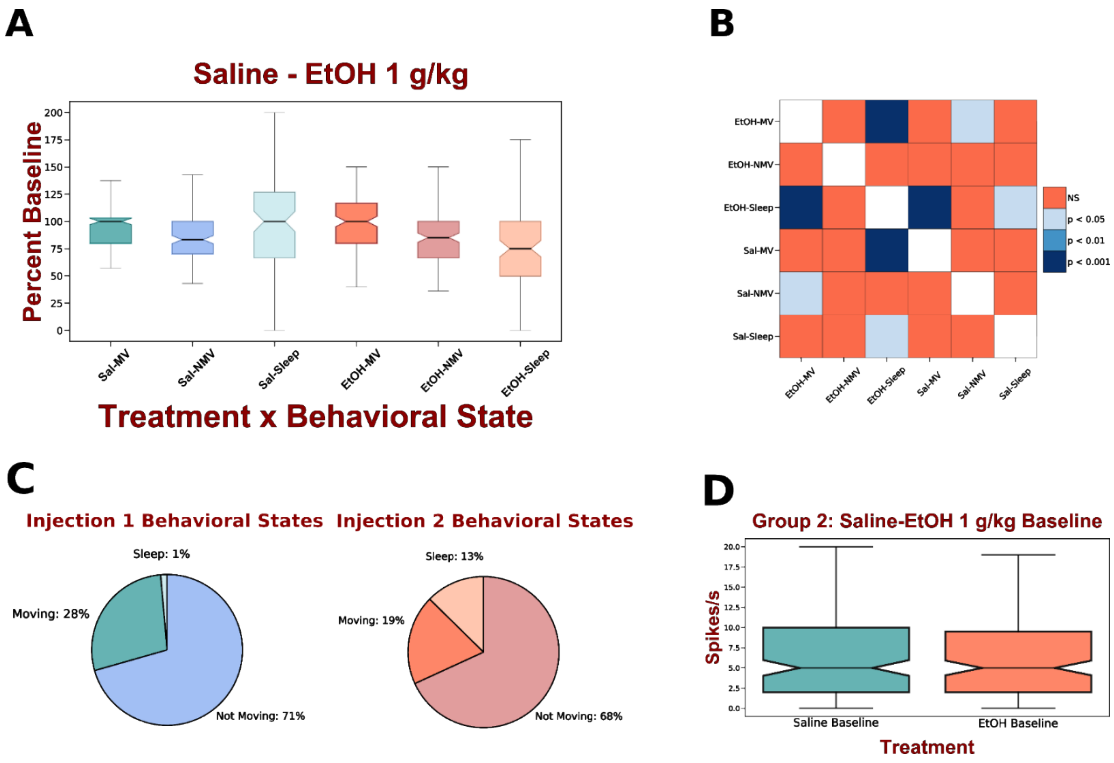

Figure 8. 1 g/kg EtOH injections reduce neural activity in lowered states of vigilance.

A. Box plots indicate distribution of baseline corrected firing rates per neuron per treatment and behavioral state. **B.** A Kruskal-Wallis omnibus test ($X^2 = 50.32$, $p < 0.00001$) was followed by a Nemenyi post-hoc test. Blue shades indicate varying levels of significance. Gross firing rates in the Saline-EtOH 1 g/kg condition are reduced in sleep and not-moving conditions. . **C**. Pie charts represent amount of time spent in each behavioral state per treatment. **D.** Comparison of baselines used to baseline normalize each treatment condition. A Wilcoxon ranked sum test indicated that baselines did not significantly differ.

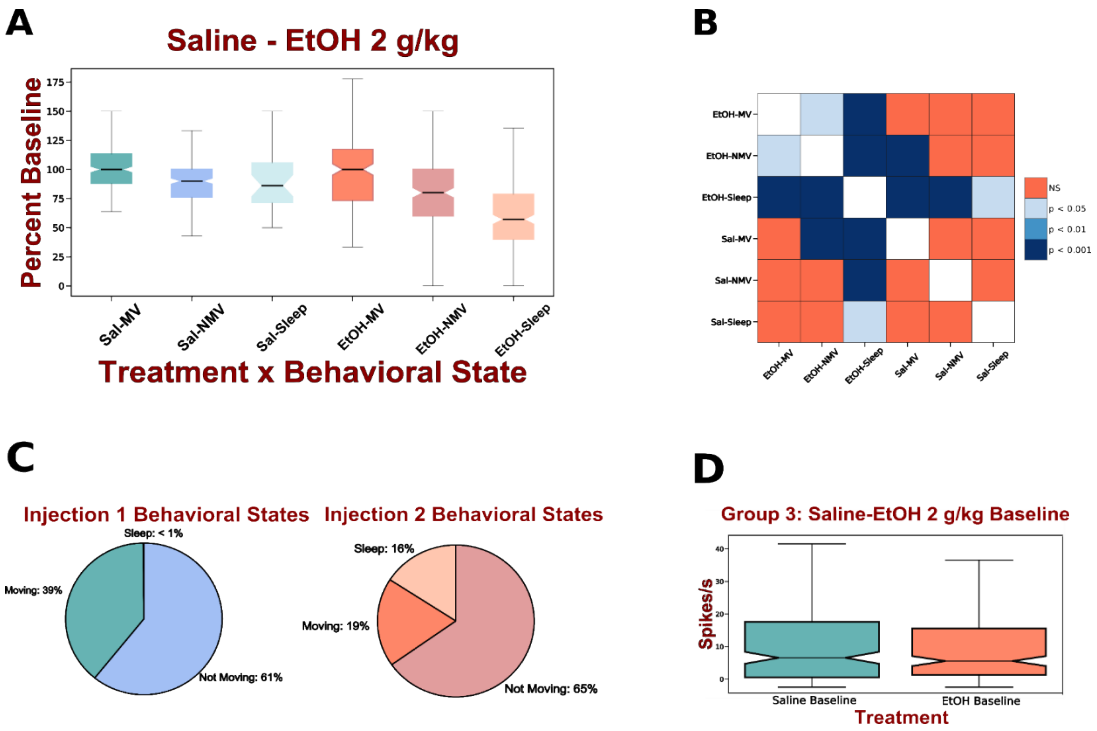

Figure 9 2 g/kg EtOH greatly reduces neural activity in lowered states of vigilance.

A. Box plots indicate distribution of baseline corrected firing rates per neuron per treatment and behavioral state.

B. A Kruskal-Wallis omnibus test ($X^2 = 181.46$, $p < 0.00001$) was followed by a Nemenyi post-hoc test. Blue shades indicate varying levels of significance. Gross firing rates in the Saline-EtOH 2 g/kg condition are reduced in sleep and not-moving conditions. Of note, the EtOH-Sleep condition is significantly different than both EtOH-MV and EtOH-NMV conditions as well as all Saline conditions.

C. Pie charts represent amount of time spent in each behavioral state per treatment.

D. Comparison of baselines used to baseline normalize each treatment condition. A Wilcoxon ranked sum test indicated that baselines did not significantly differ.

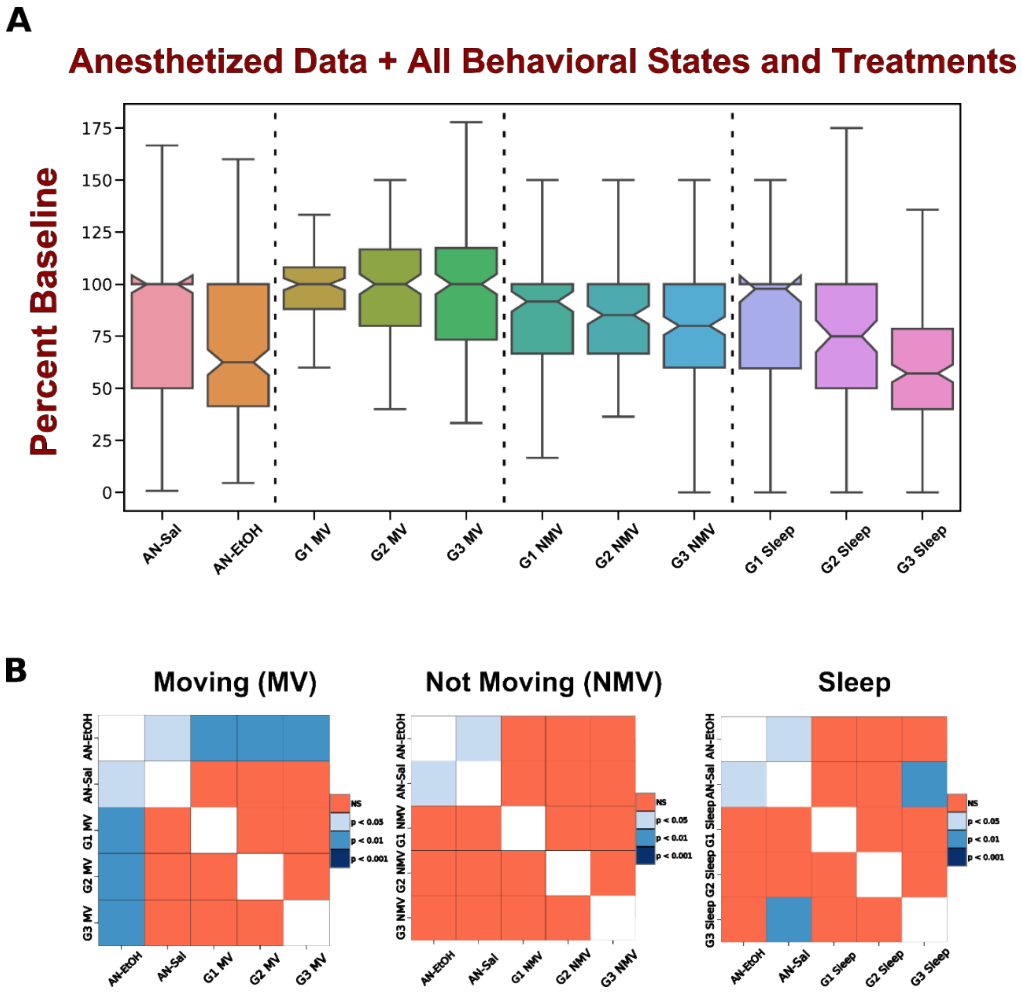

Figure 10. Reductions in neural activity comparable to anesthetized data are only found after 2 g/kg EtOH and sleep.

A. Box plots indicate distribution of baseline corrected firing rates per neuron per treatment and behavioral state. Data was separated by behavioral state and compared against anesthetized data. For example, distributions of baseline corrected firing rates in the sleeping condition were compared within each other and against both the anesthetized-saline treatment and anesthetized EtOH-treatment. There were no significant differences between anesthetized groups thus the data was collapsed (N = 582 neurons). **B.** A Kruskal-Wallis omnibus test was followed by a Nemenyi post-hoc test in each behavioral condtion. G1 indicates Saline-Saline, G2 indicates Saline-EtOH 1 g/kg, G3 indicates Saline-EtOH 2 g/kg. Firing rates in the awake-behaving condition are similar to the anesthetized-EtOH 1 g/kg condition only when the awake-behaving animal receives a higher dose (2 g/kg) and is asleep. Blue shades indicate varying levels of significance.

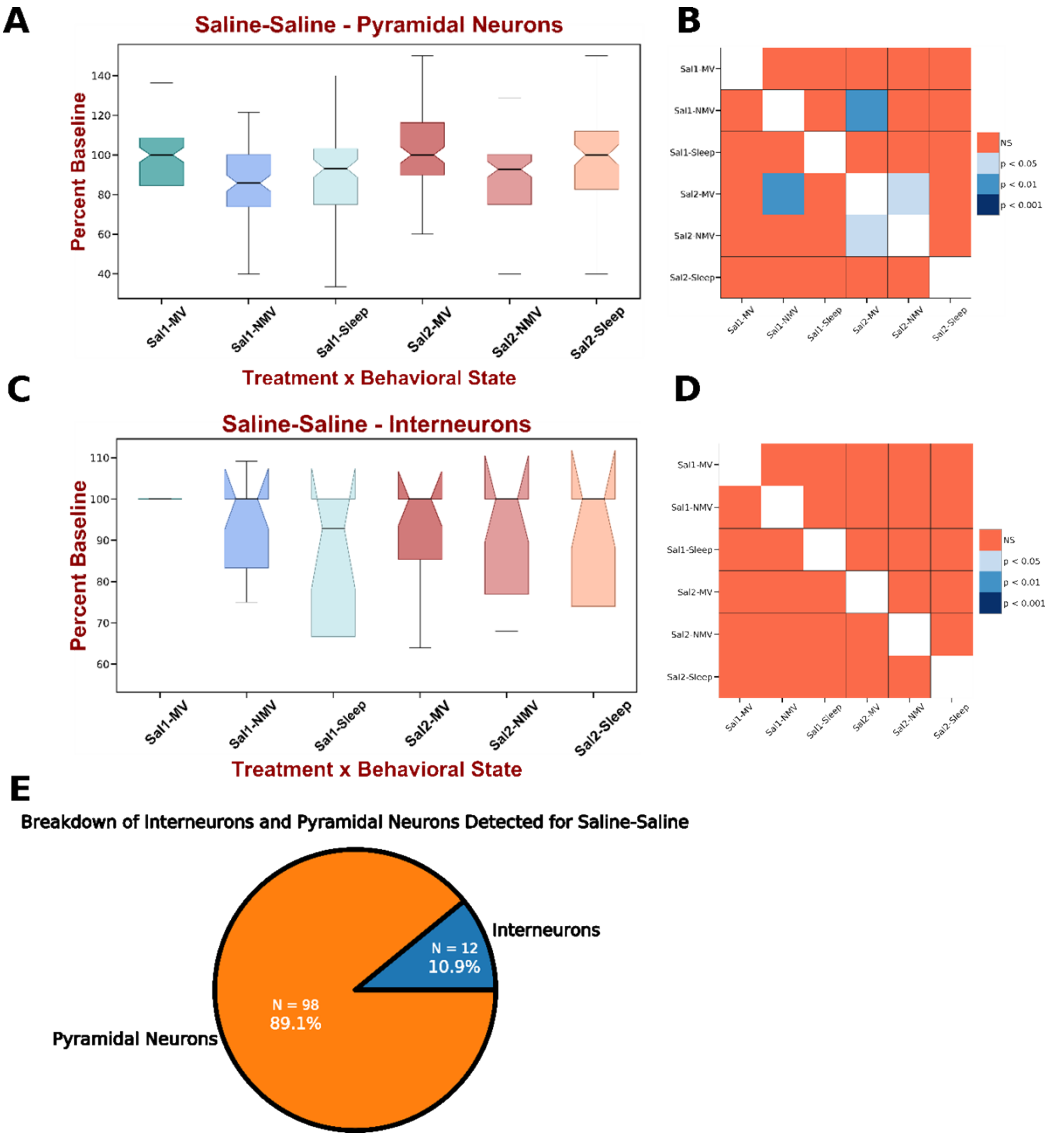

Figure 11. Comparison of interneurons and pyramidal neurons after repeated saline injections.

Group 1, Saline followed by Saline. Narrow waveform interneurons were separated from broad waveform pyramidal neurons via a classification algorithm. **A.** A significant change was detected by the Kruskal-Wallis omnibus test amongst pyramidal neurons treated by EtOH at 2 g/kg (X^2 = 24.72, p = 0.0002). **B.** This was followed by a Nemenyi's test for multiple comparisons which indicated that the Saline 2 & Moving condition was higher than the Saline 1 & NMV condition as well as the Saline 2 & NMV condition. **C+D.** No significant change was detected by the Kruskal-Wallis omnibus test amongst interneurons (X^2 = 3.14, p = 0.68).

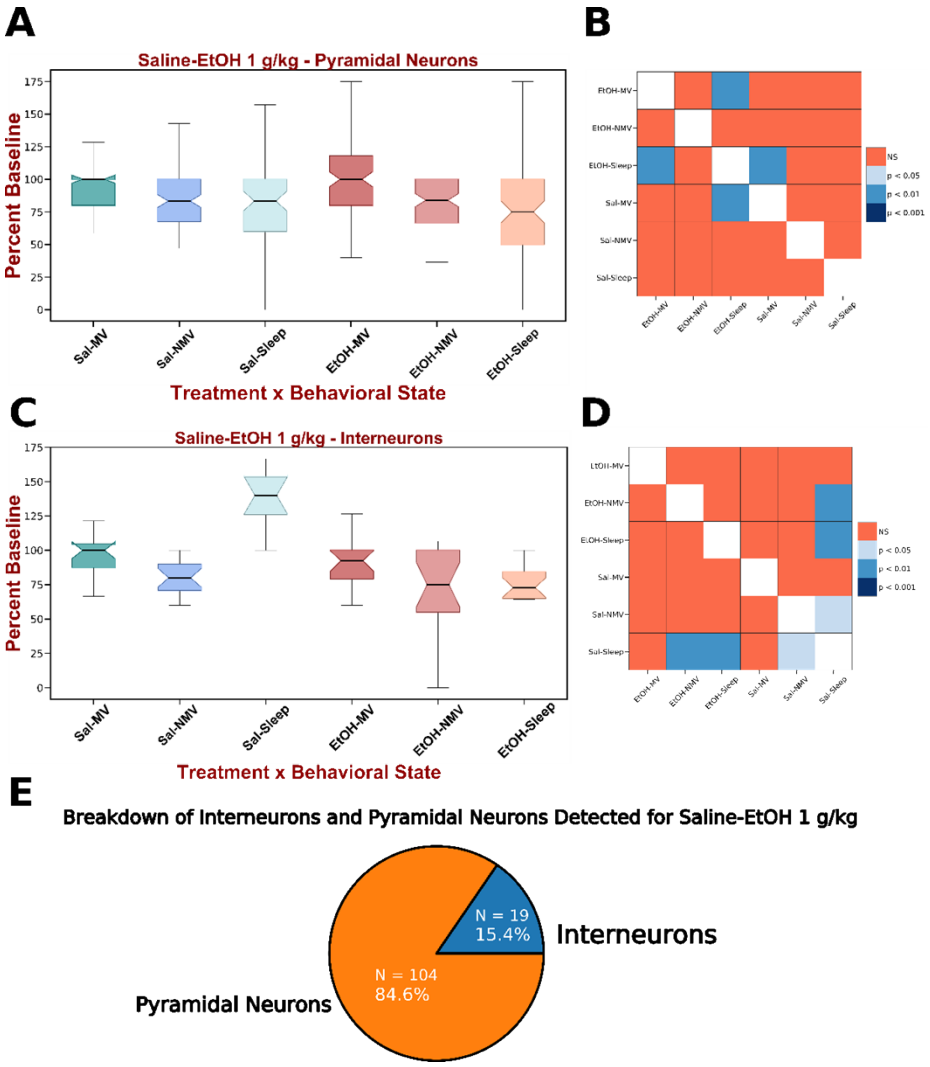

Figure 12. Comparison of interneurons and pyramidal neurons after 1 g/kg EtOH

Group 3, Saline followed by 1 g/kg EtOH. Narrow waveform interneurons were separated from broad waveform pyramidal neurons via a classification algorithm. **A.** A significant change was detected by the Kruskal-Wallis omnibus test amongst pyramidal neurons treated by EtOH at 2 g/kg ($X^2 = 35.33$, $p < 0.0001$). **B.** This was followed by a Nemenyi's test for multiple comparisons which indicated that EtOH & Sleep was different than the Saline & Moving condition as well as the EtOH & Moving condition. Additionally, the EtOH & NMV condition was significantly different than the Saline & Moving condition. **C.** A significant change was detected by the Kruskal-Wallis omnibus test amongst interneurons ($X^2 = 33.53$, $p < 0.0001$). **D.** EtOH & Sleep and EtOH & NMV conditions were significantly less than the Saline & Sleep condition.

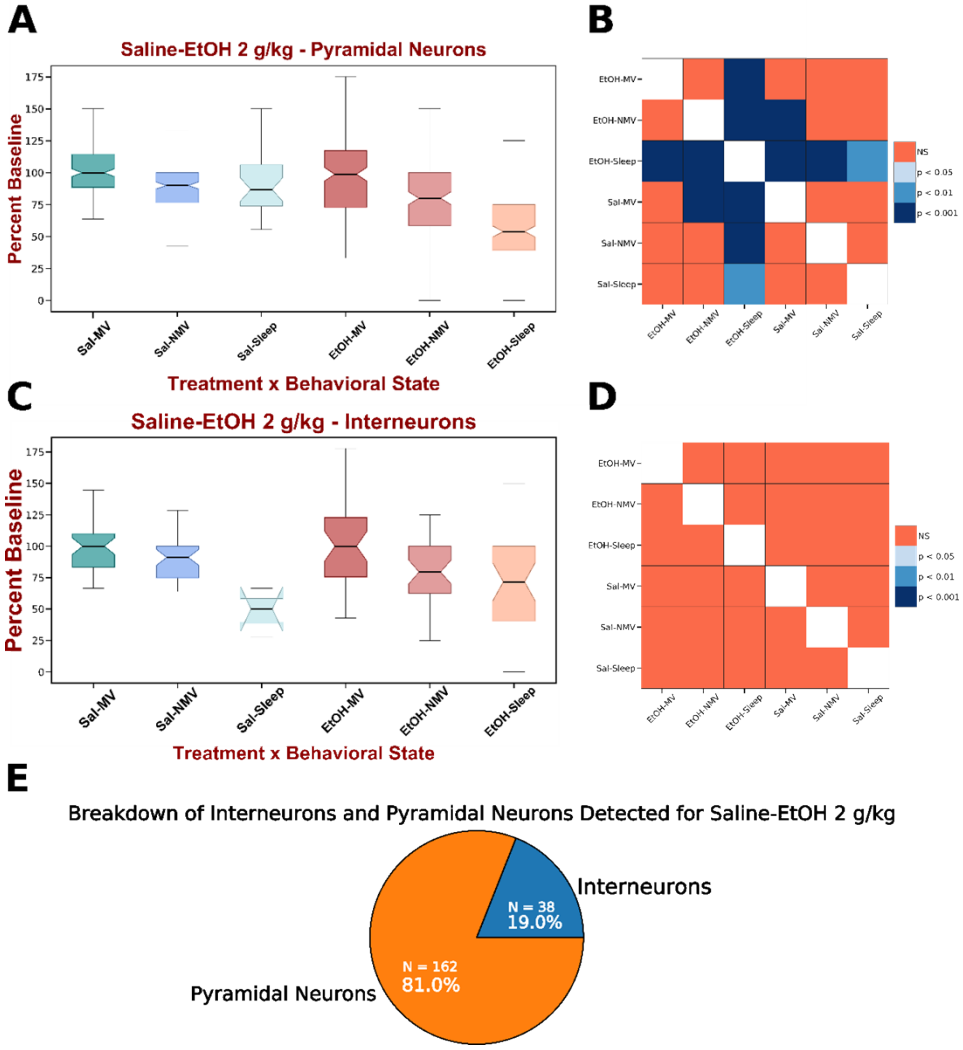

Figure 13. Comparison of interneurons and pyramidal neurons after 2 g/kg EtOH

Group 3, Saline followed by 2 g/kg EtOH. Narrow waveform interneurons were separated from broad waveform pyramidal neurons via a classification algorithm. **A.** A significant change was detected by the Kruskal-Wallis omnibus test amongst pyramidal neurons treated by EtOH at 2 g/kg ($X^2 = 168.54$, $p < 0.0001$). **B.** This was followed by a Nemenyi's test for multiple comparisons which indicated that EtOH & Sleep was different than every other condition tested. Additionally, the EtOH & NMV condition was significantly different than the Saline & Moving condition. **C.** A significant change was detected by the Kruskal-Wallis omnibus test amongst interneurons ($X^2 = 22.66$, $p = 0.0004$). **D.** However, no significant multiple comparisons were detected via Neymani's test for multiple comparisons.

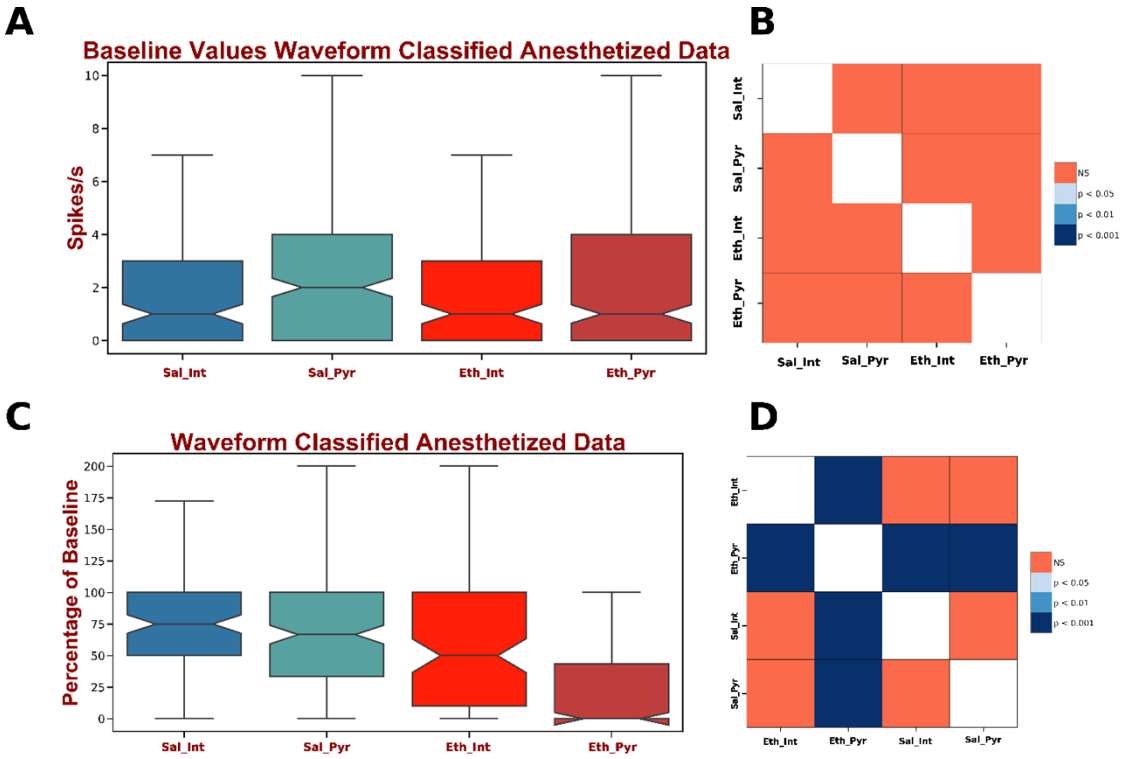

Figure 14. Comparison of interneurons and pyramidal neurons during anesthetized states

A + B. No differences were observed amongst anesthetized baselines (Kruskal-Wallis: $X^2 = 2.19$, $p = 0.53$). **C.** A significant difference was observed between anesthetized data separated by waveform type ($X^2 = 134.42$, $p < 0.0001$). **D.** After treatment of EtOH at 1 g/kg, pyramidal neurons exhibited a drastic decrease compared to every other condition (Nemenyi: $p < 0.001$). Interestingly, interneurons were not significantly different than either saline treated neuron type.

Table 1. Dataset description

Description of the dataset used for analyses prior to waveform classification. AB denotes awake-behaving, AN denotes anesthetized.

Group #	**Injection 1 (AB + AN)**	**Injection 2 (AB)**	**Injection 2 (AN)**	**#Animals (AB – AN)**	**#Neurons AB**	**#Neurons AN**
1	Saline	Saline	Ethanol (1.0 g/kg)	6 – 6	133	145
2	Saline	Ethanol (1.0 g/kg)	Ethanol (1.0 g/kg)	7 – 7	167	218
3	Saline	Ethanol (2.0 g/kg)	Ethanol (1.0 g/kg)	8 – 6	216	219